THERMODYNAMIC MODELING OF ADVANCED CYCLES FOR HIGH SPEED PROPULSION

Author
Jose Tomás Sánchez Esparza

Directors
Bayindir H. Saracoglu
Pedro Piqueras Cabrera

Von Karman Institute for Fluid Dynamics

Universitat Politècnica de València

Escuela Técnica Superior de Ingeniería del Diseño

Valencia, July 2018

Thermodynamic modeling of advanced cycles for high speed propulsion

Jose Tomás Sánchez Esparza

Von Karman Institute for Fluid Dynamics

Universitat Politècnica de València

Escuela Técnica Superior de Ingeniería del Diseño

July 2018

Choose life. Choose a job. Choose a career. Choose a family. Choose a big television, choose washing machines, cars, compact disc players, and electrical tin openers. Choose good health, low cholesterol and dental insurance. Choose fixed-interest mortgage repayments. Choose a starter home. Choose your friends. Choose leisure wear and matching luggage. Choose a three piece suite on hire purchase in a range of fucking fabrics. Choose DIY and wondering who you are on a Sunday morning. Choose sitting on that couch watching mind-numbing spirit-crushing game shows, stuffing junk food into your mouth. Choose rotting away at the end of it all, pishing your last in a miserable home, nothing more than an embarrassment to the selfish brats you have spawned to replace yourselves. Choose your future. Choose life . . . But why would I want to do a thing like that? I chose not to choose life: I chose something else. And the reasons? There are no reasons. Who needs reasons when you've got heroin?

Mark Renton - Trainspotting

Acknowledgments

I would like to express my gratitude to my supervisor at the Von Karman Institute for Fluid Dynamics for helping me so far with my project during my internship, for teaching me and giving me pieces of advice in so many topics, even not related with science and technology. To my Erasmus coordinator, Sergio Hoyas Calvo, whose dedication makes students go abroad and become more competent, efficient and better people. To Francisco Torres Herrador, for helping me in the VKI from the first minute. And finally, to my thesis supervisor in UPV, Pedro Piqueras Cabrera, for helping me with my thesis from my home university.

I would also like to thank very deeply my friends from Patrimmonia for being my family during this incredible year. Thank you all, this project has been quite easier to carry forward thanks to your hard emphasis to distract me and make me enjoy out of the master's life.

Finalmente, quiero agradecer a mi familia la oportunidad que me brindan cada día de poder lograr todo lo que me propongo. Gracias por estar siempre ahí, por apoyarme en cada decisión y en cada gesto. Sin vosotros nada de esto sería posible.

Abstract

Majority of the hypersonic and supersonic air vehicles utilizes complex propulsion systems empowered by combined-cycle engines. The architecture of such engines is quite complex to model with high fidelity methods. Transients within variety of the components throughout the trajectory play an important role on the operability and consequently on the design of the component system.

Hence, 0-Dimensional and 1-Dimensional approaches gain relevance for the conceptual design viability studies of the advanced propulsion cycles, such as air-turbo rockets, scramjets or detonation engines. The project aims to construct a framework suitable to design and simulate modern propulsion systems for high-speed transport or space access.

One of the combined-cycle engines is modeled and studied in this document. The Air Turbo Rocket, ATR, is understood as the evolution of the turbojet and the rocket engine, due to the fact that it combines components and characteristics of both of them. Moreover, it provides a unique set of features because the shaft power to the fan is independent from the flight regime, and hence from the fan performance. In addition, the ATR Expander, ATR EXP, is equipped with a regeneration system composed by two heat exchangers, one for the combustion chamber and one for the nozzle, to add heat to the working fluid, the fuel, and increase the thermodinamic efficiency.

This report focuses its efforts in the analytic research of some features of the ATR EXP in Matlab. Namely, the operational range of the engine will be studied, as well as the minimum area nozzle required for the mission, the minimum turbine work and the bleeding ratio that is necessary in supersonic regime. Apart from that, a brief introduction to EcosimPro and its environment has been made, giving examples of high speed engines studied in this numerical software.

Resumen

La mayoría de los vehículos hipersónicos y supersónicos no autónomos utilizan complejos sistemas de propulsión dotados de motores de ciclo combinado. La arquitectura de estos motores es bastante compleja como para modelarla con un alto grado de precisión. Los transitorios dentro de la variedad de los componentes que conforman el motor, a lo largo de toda la trayectoria del vehículo, juegan un rol importante en cuanto a la operatividad de la misión, y consecuentemente en el diseño del componente.

Por tanto, los métodos 0-dimensional y 1-dimensional tienen bastante relevancia en este tipo de aplicaciones, para centrarse en un diseño conceptual y de viabilidad para ciclos avanzados de propulsión, tales como los air turbo-rockets, los scramjets y los motores de detonación. Este proyecto tiene como objetivo construir un marco factible para diseñar y simular los modernos sistemas de propulsion para el transporte de alta velocidad o el acceso al espacio.

Uno de los motores de ciclo combinado se ha modelado y estudiado en este documento. El motor Air Turbo Rocket, ATR, está considerado una evolución del motor turbojet y el motor cohete, debido al hecho de que combina tanto componentes como características de ambos. Además, proporciona una serie de características únicas, ya que la potencia del eje que se da al fan es independiente de la condición de vuelo, y por tanto, del rendimiento del fan. Adicionalmente, el ATR Expander, ATR EXP, está equipado con un sistema de regeneración compuesto por dos intercambiadores de calor, uno para la cámara de combustión y otro para la tobera, que proporcionan calor al fluido de trabajo, el fuel, para así incrementar la eficiencia termodinámica del ciclo.

Este trabajo focaliza sus esfuerzos en el estudio analítico de algunas características del ATR EXP en Matlab. Concretamente, se estudiará el rango operacional del motor, así como también el área mínima de la tobera requerida para la misión, el trabajo mínimo que debe hacer la turbina, y el coeficiente de sangrado que debe existir para régimen supersónico. Aparte de eso, se hará una introducción breve a EcosimPro y su entorno, dando ejemplos de motores de alta velocidad estudiados en este software numérico.

Nomenclature

A transversal area $[m^2]$

a speed of sound $[m\ s^{-1}]$

B bypass ratio $[-]$

C_h constant specific heat capacity $[m^2 s^{-2} K^{-1}]$

C_p heat capacity at constant pressure $[m^2 s^{-2} K^{-1}]$

D diameter $[m^2]$

D_h hydraulic diameter $[m^2]$

e total energy $e = H - p\nu [m^2 s^{-2}]$

G mass flux $[kgm^2 s^{-1}]$

g gravity constant $[m^2 s^{-2}]$

H total enthalpy $H = h + 0.5\nu^2 [m^2 s^{-2}]$

h enthalpy $[m^2 s^{-2}]$

h_c convective heat transfer coefficient $[m^2 s^{-2}]$

I_f fluid equivalent inertia $[m^{-1}]$

I_v valve equivalent inertia $[m]$

I_{sp} specific impulse $[ms^{-1}]$

K thermal conductivity $[kgms^{-3} K^{-1}]$

K_f pressure loss factor $[-]$

q heat $[m^2 s[-2]]$

T temperature $[K]$

T thrust $[N]$

T_{sp} specific thrust $[Ns^{-1}]$

v velocity $[ms^{-1}]$

W Work $[kgm^2 s^{-2}]$

Ma   Mach number

Nu   Nusselt number

Pr   Prandtl number

Re   Reynolds number

Acronyms

ATR   Air Turbo-Rocket

ATREX Air Turbo-Ram-jet wit Expander engine

CFD   Computational Fluid Dynamics

DAE   Differential Algebraic Equation

DASSL Differential Algebraic System Solver Algorithm

DMR   Dual-Mode Ramjet

ESA   European Space Agency

ESPSS European Space Propulsion System Simulation

HAP   Hypersonic Air-Breathing Propulsion

HSI   High Speed Intake

LSI   Low Speed Intake

MR   Air-to-Fuel Ratio

RBCC Rocket Based Combined Cycles

SABRE Synergetic Air-Breathing Engine

TIT   Turbine Inlet Temperature

TPR   Total Pressure Recovery

TSFC Thrust Specific Fuel Consumption

TSTO Two Stage to Orbit

Greek Symbols

α_c intake mass capture ratio

Δ increment

δ_p pressure loss

ϵ_r wall rugosity $[m]$

η_n nozzle efficiency

η_o overall efficiency

η_p propulsive efficiency

η_{th} thermal efficiency

γ heat capacity ratio

ν dimensionless velocity

π compression ratio

ρ density $[kgm^{-3}]$

τ characteristic time $[s]$

ξ friction factor $[m^{-1}]$

Superscripts

o   stagnation quantity

Subscripts

∞ free stream

a   air

amb   ambient

cc   combustion chamber

crit   critical condition

f   fan

h   hydrogen

N   net

n   nozzle

p   pump

t   turbine

Other Symbols

ΔH specific work $[m^2 s^{-2}]$

$\dot{m}$ massflow $[kgs^{-1}]$

$\dot{q}$ heat flux $[kgs^{-3}]$

$\mathcal{F}$ thrust $[kgms^{-2}]$

x

Contents

List of Figures

List of Tables

Introduction

1.1 High speed propulsion context

1.1.1 High speed propulsion and its environment

High speed propulsion is becoming nowadays a challenge in which thousands of engineers are working on, making big progress and achieving goals to make possible high speed propulsion as a fact in the long-term future. In order to accomplish this objective, some programs are being carried out by the main agencies in aerospace investigation, such as the European Space Agency, ESA, with its program LAPCAT, Long-Term Advanced Propulsion Concepts and Technologies.

For developing an efficient propulsion plant that is able to travel at supersonic or even hypersonic velocities and whose applications will be focused on commercial flights or space access, there are some tasks to deal with: the airframe and the optimization of the propulsion unit. When the trajectory analysis is being studied, its common to presume the performances of both the airframe: drag, lift, thrust, fuel consumption, etc.; and the propulsion plant, which are required to accomplish the mission. In turn, the airframe and the propulsion unit are designed assuming performances too, and then the mission is imposed on the performances calculated when overcoming this step. The separated design of these areas from the general system is often performed in subsonic airplanes and applications, which constitute problems in which installation and interaction effects are less sensitive to the operational range and flight regime. Nevertheless, components become more delicate when flying at supersonic regime, e. g. the intake is a critical component, due to the fact that it has to deal with lots of different scenarios of velocity and ambient conditions, so its range of operation has to be very wide in order not to establish a mismatch between it and the downstream components like compressors, and then provoke a huge loss in efficiency, specific thrust and consumption, etc. That's why it is very important, even more in supersonic and hypersonic regime, the address of the total interaction between components and between the propulsion unit and the airframe from the very early design stages.

The propulsion unit design include complex challenges that need to be overcome. Despite the effort employed in ramjet and rocket engines, the High Air-Breathing Propulsion, HAP, technology presents disparities related to its flight regimes that have no easy solutions. It may exists a solution for one flight speed corridor, but that is not good for the other ones. Then, it is been suggested to combine different propulsion systems in order to facilitate the engine operation at different flight speeds with different modes of propulsion. For instance, the Turbine Based Combined Cycle, TBCC, join both the turbine and the ramjet/scramjet systems. In this framework, the turbine cycle is used to drive the aircraft to flight speeds in which the ramjet/scramjet unit can be ignited and then used to reach and maintain the hypersonic regime. Nevertheless, TBCC cycles contain multiple difficulties of implementation, as the transition through the different propulsion cycles and the effective integration between them [3]. Advancements in this area are needed, and this is in turn subdivided in several areas of investigation, such as:

- Air breathing engines:

  - Dual-mode ramjet/scramjets, DMR.
  - High speed turbines
  - Rocket based hypersonic flight; limited success with ramjet missiles at subsonic to supersonic speeds.
  - Operational hypersonic vehicle even with much work done in ramjets and scramjets.

- Rocket propulsion:

  - Improvements to liquids, solids and hybrids used in RBCC or booster stages.
    – Combustion inestability.
    – Internal flowfield modeling.
    – Components; nozzles and turbomachinery.
  - Booster stages to make them more efficient and cost effective.
    – Flight testing.
    – TSTO system.

- Combined cycles:

  - Turbine based combined cycles, TBCC,
    – Variable geometry.
    – High speed turbines and turbojets.
    – Transitioning and integration.
    – Materials.
    – Thermal management.
    – Engine components.
  - Rocket based combined cycles, RBCC,
    – Rocket-scramjet integration.
    – Linear aerospike rockets and nozzles.

- Compressor and turbine blades.

- Engine components.

  - Seals.
  - Turbomachinery.
  - Seals.

- Fuels and combustion.

- Heat management.

- Engine performance.

- Flow paths:

    - Intake.

    - Isolator.

    - Combustion chamber.

    - Nozzle.

    - Structure.

    - Acoustics.

As this list suggests, there is a huge amount of remaining work to make high speed propulsion based on combined cycles a reality. This document is going to be focused just on describing, modeling and studying one type of the combined cycle engines, the Air Turbo-Rocket, ATR, but first a review of hypersonic vehicles is introduced.

1.1.2   Hypersonic vehicles

There are several ways to classify hypersonic vehicles, and one of the most interesting ones is by their propulsion plants. Vehicles with a single type of power plant usually uses either variable or multimodal cycle engines. Vehicles using a combination of power units base its operational work on different engines, depending on the flight phase. A representation of this concept could be a turbo-ramjet combined with several rocket engines to thrust up the Sänger two stage to orbit, TSTO, vehicle [4], [5], and a cycle composed by an ATR and a DMR to power up the LAPCAT II Mach 8 civil transport vehicle. On its behalf, multimodal engines are capable of modifying their configuration to accomplish the best efficiency at each stage of the flight. This is a concept represented by the Synergetic Air-Breathing Engine, SABRE, designed for launching the Skylon by a single stage to orbit, SSTO, mission [6], [7], and the Scimitar, for the LAPCAT A2 Mach 5 vehicle [8], [9].

Designing a high speed air-breathing cycle engine is an assignment in which there exists a trade-off to be followed between the specific impulse, thrust-to-weight ratio and operational envelope. The specific impulse is a very useful parameter to measure the cycle efficiency, due to the fact that is defined as the thrust generated by the engine divided by the fuel mass flow it consumes. TBCC are very effective to maximize the specific impulse in this kind of missions, so that's the reason why the majority of engines related to this technology are based on these components.

1.1.3   Cycles designed for high speed propulsion

The propulsion cycles thought to achieve the high speed regime are differentiated in three main categories, depending on the implementation of TBCC, RBCC or a ramjet/scramjet based cycle.

The TBCCs are composed of the turbojet and the ramjet cycles, particularly turbo-ramjet (Griffon II engine [10] and Sänger) and turbofan-ramjet (RTA-GE57, evolution of J58 engine from the SR71 Blackbird [11], [12]). Variants of this technology comprehend the modifications of the classical turbojet configuration, the ATR [13], [14] and the ATREX (Air Turbo-Rocket Expander) [15], a pre-cooled ATR. There are other configurations, such

as the MIPCC engine [16] and the Rocket Augmented Turbine [17] which include some modifications to the turbojet cycle to provide some specific performances.

The RBCCs are based on combinations of air-breathing and rocket elements. For instance, SABRE, Scimitar, KLIN, RB-545 and GTX engines [7], [18], [6]. SABRE and Scimitar engines are similar to the ATR in the core, but with a combustion chamber and a nozzle characteristic of rocket systems.

Finally, the ramjet/scramjet engines have a particularity: they do not provide static thrust, so they need to be accelerated by other propulsion plant. Consequently, the booster and the engine are integrated to achieve a good configuration. If desired, more information about this type of cycles is available in [7], [18], [6], [19].

1.1.4 Air Turbo-Rocket engines

Within the ATR technology, there are two distinguished categories depending on the source of the hot gas driving the turbine. The configuration in which this document is focused is called the EXP one: the combustion is carried out just in one single combustion chamber, and the turbine is driven by regeneratively heated fuel extracted from this single chamber and from the nozzle. The second category, the gas generator, GG, is based on a pre-combustor burning a rich mixture of on-board oxidizer and fuel to generate the hot gases which are going to discharge to the main combustion chamber that mixes these gases with the air coming from the atmosphere.

NACA designed an ATR-GG in 1956 [13], based on gasoline as fuel and nitric acid as oxidizer, with a driven fan through a gearbox and a partial admission turbine. The optimum condition was established to Mach 2.3 and 14 km of altitude. When the supersonic cruise is taking place, the fan is windmilling and then the engine is behaving as a ramjet engine. During the 60s other concepts of ATR-GG were patented, as well as EXP configurations were starting to be developed [20], [21].

SNECMA developed in 1992 an ATR-GG combined with a ramjet engine. It was based on two counter-rotating fans driven by two contra-rotating turbines, and there was H_2 cooling to the fan blades when the flight speed exceeded Mach 3. As the speed increases, the blades change its position by pitch control to make the transition to ramjet mode.

The ATR EXP started its development thanks to the investigations carried out by ASTRIUM [22] and SNECMA [23], based on preliminary data extracted by ESTEC [24].

1.2   Project goals

There are several objectives that will be accomplished in the developing of this project:

- Documenting and studying high speed propulsion engines constitutes the first objective of the project, due to the extensive background that exists and that constitutes the starting point of the current work. An exhaustive compilation of information will be made, studying engines such as the SABRE, the Scimitar and the ATR-EXP. Nevertheless, the main goal of the project is studying this last engine, so understanding this engine, its meaningful parameters and its behavior when some conditions have changed will be necessary.

- Learning and understanding the software EcosimPro will be the second objective. As next sections will describe, this software constitutes the perfect tool for modeling high speed propulsion engines.

- Being able to develop some studies about turbojet and ramjet engines in EcosimPro, and its homologous in some other software such as Matlab and GasTurb for future comparisons and validations will be the third objective, proving that the student has acquired the sufficient knowledge for modeling high speed propulsion engines.

- The final objective of the project is focused on studying in Matlab the high speed propulsion engine ATR-EXP, Air Turbo Rocket - Expander. The utilization of this software is due to its capability of performing studies faster than EcosimPro, being able to obtain tendencies, behaviors and conclusions that will be used for more specific studies in EcosimPro. Thus, this studies will be used for obtain the meaningful parameters of the engine, focused on the turbomachinery cycle. Besides, the operational range of the engine will be obtained, and once this framework is calculated, several studies analyzing behaviors when some parameters have changed, such as the bleeding, the nozzle area or the turbine specific work, will be carried out. Similar studies in EcosimPro, in which the accuracy of the model will be increased considerably, are proposed for future works.

The Numerical Tool: EcosimPro

The methodology followed in this document will be presented below. For the realization of the different studies that have been developed in this project, some numerical tools have been used. These tools allows the user to analyze the engine in its several states of working, such as design, off-design and transient conditions. In the design phase, the calculus focuses on the determination of the geometry and the cycle for a specified mission. Then, the off-design operation is analyzed to study the engine behavior throughout its operational range. Finally, the transient stage is the most complex one, due to the fact that it combines the off-design state of all components which integrate the engine, plus the transient term of the governing equations.

In order to study these three states of operation, the simulation environment Ecosim-Pro has been used, combined with the European Space Propulsion System Simulation (ESPSS) libraries, which include all the components needed to build the engine models.

2.1   A general introduction to the software

As commented before, EcosimPro is a simulation tool developed by Empresarios Agrupados which counts on an user-friendly environment destined to model both simple and complex physical processes that are declared either as systems of differential-algebraic equations or as ordinary-differential equations, combined with discrete events.
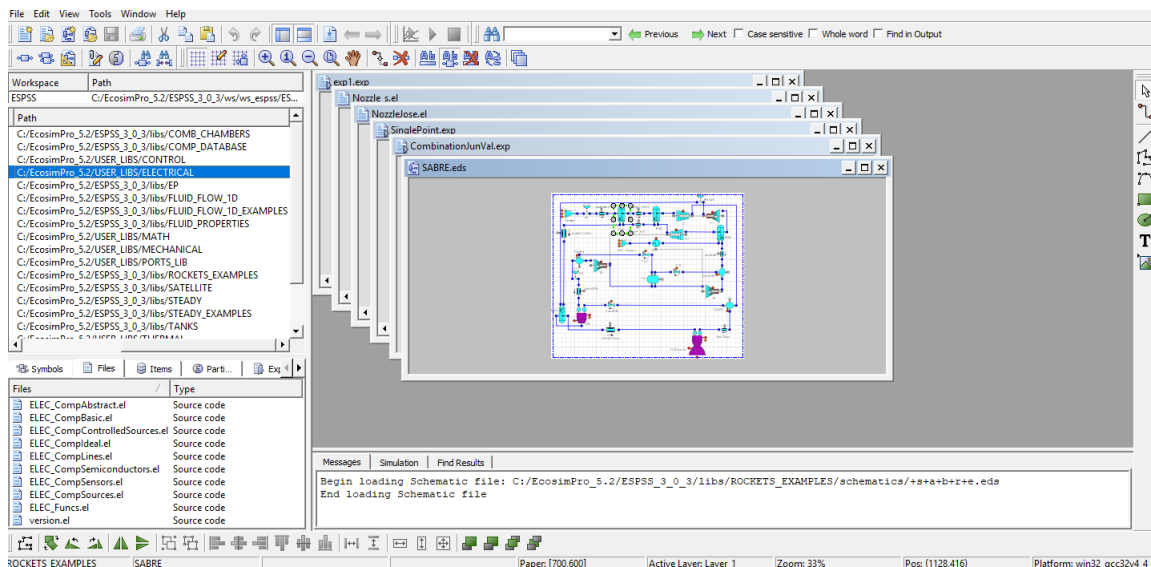

Figure 2.1: EcosimPro software - general view

EcosimPro employs a specific programming language named EL, which is thought to model physical systems based on discrete events and equations. This language is the official one utilized by the European Space Agency (ESA) and it permits the mathematical modeling of physical components by representing them through differential-algebraic

equations. The goal of the EL developing is modeling combined continuous and discrete systems, doing it in a clear and easy way.

EL is a very powerful tool that is used in applications such as preparing experiments, calculating design points and off-design behaviors, transient processes, etc. It is not only useful for developing models and computing them, but also for the post-processing task, by generating plots, reports, and compatible data with other languages like FORTRAN, C and C++.
This language is designed to solve systems of differential-algebraic equations automatically. Nevertheless, the complexity is hidden internally, where the system is solved: the user has to define the high-level equations by using a high-level object-oriented language that is very similar to other object-oriented languages. Consequently, in EL language components have the capability to inherit properties, equations and variables from other object, and in turn can be established as a base for creating a more complex object or system. As a matter of fact, these characteristics allow the user to be able to create big, high complex models that can go from a simple electric circuit to a huge engine designed for a space mission.

There are many concepts in EcosimPro, but the most important ones are:

- Workspaces: A workspace consists on a combination of libraries the user is going to use in its simulations and experiments. The libraries can be included, deleted or created, depending on the necessities of the project. Alternatively, the user can create different workspaces with different configurations and libraries if desired.

- Libraries: Libraries are sets of elements related to the same area of study, stored in one unique file. In a library, multiple kinds of elements can be included, such as components, variables, constants, functions, ports or classes. An important property of this type of units is that they can interact in between with other libraries, due to their multi-disciplinary constitution.

- Components: These concepts are the most important ones in the whole modeling task. A component represents a physical unit, like a compressor, a turbine, a valve, etc., and it models as well its discrete, continuous or sequential behavior, depending on the case study. A component can be connected to other components to create general systems, which are going to be computed for different goals and purposes. For instance, an inlet could be connected to a compressor, a combustion chamber, a turbine and a nozzle to build up a turbojet engine model.

  There are two categories: concrete and abstract components. The last ones are used just to join sets of variables, discrete events and equations, and have no real significance. Abstract components are inherited by others, establishing a parent-and-children structure in which children use the data from a general parent. It provides simplicity to the code, since it is well structured and avoid repetition.

- Ports: These units represent the connection between components. There are several categories of ports, and the user can create them and choose its category depending on the necessity of the model [25].
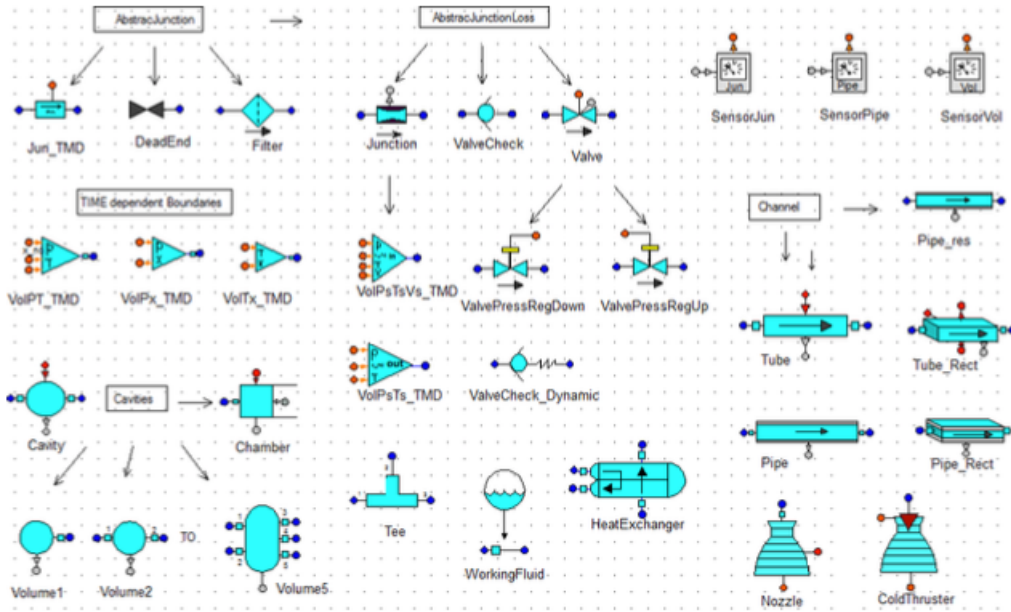
Figure 2.2: Example of library "Fluid Flow 1D" with all its components [1]

Actually, ports exchange variables between the components they join. The main advantage of working with this type of element is that no connection between variables is needed, because the port is the one in charge to transmit data from one component to the following one. Ports have several properties, such as the type of data they work with (Real, boolean, etc.), the type of connection (equal, sum, etc.), and the direction (in or out). In turn, there are several categories of ports, depending on what is being transported; fluid, thermal energy, control data, etc.

- Partitions: Once the system is made by choosing and connecting the components, the mathematical model has to be created by ordering the equations, choosing the boundary and initial conditions, and proposing a set of residue equations and tearing variables. Partitions are exactly this process, and for a single model several of them can be created, by choosing different boundary conditions, different unknown variables, etc.

- Experiments: Once the partition is created, experiments are the next step in the pre-process stage of the simulation. They are created to define the correct use of the model, by specifying the initial state of the system, the boundary conditions, integrating the model between an initial and a final time and choosing the step, choosing whether doing a steady or a transient calculus, etc.

Regarding the mathematical capabilities of EcosimPro, the software works with symbolic equations (derivatives, reduction, etc.) and numerical solvers for differential-algebraic equations (DAE) such as Runge-Kutta and DASSL, Differential-Algebraic System Solver algorithm, and non-linear equations (Newton-Raphson) [26]. The program automatically controls the interaction between these solvers, and uses sparse and dense matrix formats which change in function of the Jacobian matrix, in order to deal with thousands of vari-

ables that take part in the mathematical model [27].

When creating a partition, the numerical tool is provided with wizards for defining design problems, establishing boundary conditions, overcoming algebraic loops and reducing DAE problems.

Given a non-linear system of equations as the following one

$$\begin{cases} F(\dot{x}, x, t; u) = 0 \\ \quad x(t_0) = 0 \end{cases} \tag{2.1}$$

For the resolution of this system of equations, the Differential-Algebraic System Solver algorithm (DASSL) for implicit systems is used. DASSL results very useful when two types of problems need to be solved, and cannot be handled by other ODE solvers. Contrary to Runge Kutta method, for instance, it is not necessary that the derivative is in explicit form. Another type of DASSL can be used in EcosimPro, which is the DASS-SPARSE solver. It is used when the Jacobian is very large, with a high number of zeros. By using the SPARSE option, the calculation time is reduced considerably. The advantage of using DAEs is that when modeling a physical system, the originated equations are DAEs themselves, and not ODEs. ODEs are special cases of DAEs, so an ODE can be written explicitly as a DAE.

The solver used by EcosimPro (DASSL) consists on a method in which the time derivative $y'(t)$ is replaced with an approximation by differences, and the resulting equations for time are solved by using an implicit Powell's Hybrid Method, by iterations. Then, the algorithm replaces the time derivative not only using first order approximations, but also by using a backward differentiation of order, where k is between 1 and 5. The value of k and the time step are parameters chosen automatically by the solver at each step, based on the behavior of the solution. As mentioned before, the implicit iteration technique is a Powell's Hybrid Method. As in any other method, the vector of unknown variables requires a set of starting values. The convergence is obtained faster when these values are close to the solution ones. The DASSL algorithm estimate the starting values, evaluating the interpolation polynomial for the solution calculated the last $k+1$ times at the current time t_n.
If the initial conditions are inconsistent, the solver may diverge. This difficulty is observed when creating large algebraic systems by introducing algebraic compatibility equations between different components. To solve this problem, the order of the algebraic constraints has to be reduced through the implementation of the perturbed equation. In the case of the components that take part in an ATR engine, this perturbed equation corresponds to the compatibility of mass between two connected components, named by 1 and 2.

$$\dot{m}_1 - \dot{m}_2 = \tau \ddot{m}_2 \tag{2.2}$$

This equation replaces the original stiff equation which was obtained when the characteristic time was approaching to zero. By this measure, the system of equations will be split in two separated parts, and will be solved independently.

2.2   The object oriented modeling

When building up models composed by a set of components, object-oriented languages constitute a powerful tool to avoid complexity and leverage the code reuse, in order to create models which can be independent and whose maintainability is considerably easy. The development based on modular procedures makes possible the creation of complex models by combining two methods:

- Using existing components and inherit them by extension.

- Aggregating and instantiating existing components.

These methods are thought to create components that are able to represent real and entire physical systems. Nevertheless, single or intermediate components could be simulated as well (a turbine, for instance, could be simulated by aggregating some components to study its performance, it is not needed to simulate big systems as turbojet engines to study the behavior of one single component). The development of the model and the maintenance time that are needed for consistent results are critical tasks that are optimized with some important tool

- Encapsulation: Encapsulation of complexity is one of the goals of an object-oriented language and modeling. Both the abstraction capability and the encapsulation of data are very efficient ways to make the process much simpler. The main elements to carry out this task are components and libraries.

  For instance, a certain user could build a model in which there are hundreds of variables and equations that may work properly, but when other user wanted to read it, it could become difficult to follow and understand. The libraries include all the elements which are part of one subject, and the components constitute the fundamental unit for expressing a dynamic behavior by modeling its physical state and operation. Their public interface lie in its data, ports and construction parameters, and are visible for the user when the modeling phase is being carried out. The port includes variables for connections to the components, and they transport also the behavior and restrictions between ports. The definition of different classes of ports abide in the system is capable of insert connection equations for the user not to be concerned about them. If desired, the user could add some new components without being worried about the connection equations but their internal behavior, because the connections between ports are the ones in charge to determine whether the union is possible or not.

- Inheritance: This is the tool employed for provide EL language of power for sharing behavior and interfaces. When many components are used in the same model, they may share a quite similar behavior. In order to simplify the mathematical model, the language could deliver equations and data from the parent component to the children ones, in order not to extend the model with similar equations and variables. As a matter of fact, libraries are created by defining a parent component and then inheriting its properties to other children, which will have the same properties than its father, and then changing the code and including new features to specify the behavior of this last component. Moreover, the software allows multiple inheritance;

a component could be created by taking properties from several parents, so the creation of new components by using different parts of other ones is allowed.

- Aggregation: As commented before, a component can be created by inheriting properties from other one or ones. As well, they can have some instances of other components, in order to increase the feature of reusing code and properties, since the new component is based on others already built up.
  If the language apply this principle iteratively and without any limit, the final component could have a huge complexity, due to the large quantity of equations it includes. Nevertheless, this complexity is internally hidden by the aggregation of previously verified instances of other classes.

- Data abstraction: The language provides numerical data such as INTEGER, FLOAT or REAL, and other convenient data as STRING, for instance.. As well, it includes the possibility of defining user's own data types [28].

2.3   Classes

In EL language, classes are quite similar to the ones present in other object-orientated languages, such as Java or C++, but with one fundamental difference: EL is more restrictive, because it is simpler. It must be taken into account that users of this program are engineers, not programmers.

This language gives the user the possibility to encompass data and behavior in the same item, and then call it in a certain model to use it. The difference between a class and a component is that the second one is equipped with dynamic equations and discrete events that will be solved by the numerical tool. On its behalf, a class just depicts a certain behavior, and only permits the declaration of methods and variables.

Classes are usually employed when the user want to model complex systems where exists the possibility of improving the use of functions if they are referred to a similar utility, so they are stored together and share memory by using similar variables.

2.4   The ESPSS libraries

EcosimPro is a software destined to model and calculate simple and complex physical systems modeled by mathematical equations. In order to do this, an object-oriented programming language is created, and its base, the components, are stored in libraries which include equations, variables, ports, classes, etc., as commented before. The European Space Propulsion System Simulation is an ESA initiative focused on the creation of a platform for the spacecraft and launch vehicle propulsion systems simulation. Namely, it is formed by a set of libraries designed for taking part in the numerical software Ecosim-Pro. In order to provide real, consistent results, the libraries have to be updated with the state-of-art technology at the time they are used for analyzing phenomena mainly focused in propulsion systems.

The group in charge to create ESPSS and EcosimPro was composed by four companies: Empresarios Agrupados, which are the ones under the care of coordinating the project

and modeling ESPSS; CENAERO, responsible for developing the 1D algorithms, zooming with CFD codes and system optimization, since it is a company specialized in CFD and Optimization methods; EADS Astrium Space Transportation, in charge of creating the User Requirements and Validation cases; and finally KOPOOS, responsible for the Tank filling and Priming validation cases, since it is an enterprise with experience in satellite propulsion systems, both with chemical and electrical power [29].

These libraries count on several tools designed to model propulsion systems features such as:

- Standard properties for pressurant, propellant and some other fluids and materials, taking into account the possibility of creating new ones by the user.

- A general fluid 1D model for two phase flows, destined to systems where heat transfer takes place or controllers are needed.

- Libraries to model 1D turbo machinery and tanks behaviors.

- Combustion chambers, nozzles and cooling systems libraries.

It is remarkable that ESPSS includes a library focused just on steady components; obviously, it is not the same to model a compressor actuating in its steady behavior or in its real one, taking into account parameters like inertia, time delays, etc. Then, ESPSS contemplate that possibility and provides libraries not only for real behavior, but for steady one too. Having said this, the main applications for these libraries are the modeling of:

- Spacecraft systems, including processes of prime, heat transfer, tank behavior, pressure regulators, etc.

- Ground pressurization systems.

- Priming phenomena, calculated in pipes or in other subsystems that are not the main problem in spacecraft general systems.

- Liquid rocket engine cycles with one or several burners, including turbo machinery and cooling systems. This is the application in which the present document is going to be focused.

The circulating flow across the linear components, doing it in a one-dimensional way, is resolved by the governing equations of mass, momentum and energy as:

$$\frac{\partial \omega}{\partial t} + \frac{\partial f(\omega)}{\partial x} = \Omega(\omega) \tag{2.3}$$

where the terms ω, $f(\omega)$ and $\Omega(\omega)$ are the conservative variables, flux and source terms, respectively.

$$\omega = A \left\{ \begin{array}{c} \rho \\ \rho \nu \\ \rho e \end{array} \right\}$$

13

$$f(\omega) = A \left\{ \begin{array}{c} \rho\nu \\ \rho\nu^2 + p \\ \rho\nu(e + p/\rho) \end{array} \right\}$$

$$\Omega(\omega) = \left\{ \begin{array}{c} 0 \\ \frac{1}{2}\xi\rho|v|A + p(dA/dx) \\ \dot{q} \end{array} \right\} \tag{2.4}$$

The source term of the equation of energy, $\dot{q}$ is related to the heat transfer coefficient, h_c, related to convective effects, and it can be rewritten as:

$$\dot{q} = h_c \ (T_w - T) \tag{2.5}$$

where T_w and T corresponds to the wall and fluid temperature, respectively. As well, a correlation to represent the heat transfer mechanism is needed, and it is modeled by the Nusselt number, which is in turn utilized to compute the convective heat transfer coefficient:

$$h_c = Nuk/D_h \tag{2.6}$$

$$Nu = f(Re, Pr) \tag{2.7}$$

where D_h is the hydraulic diameter of the section. The friction factor, which will model the pressure loss per unit of length in pipes and ducts, is computed using the correlation by [**20Churchill**]

$$\xi = K_f/D_h \ f(Re, \epsilon_r/D_h) \tag{2.8}$$

$$f(Re, \xi_r/D_h) = 8((8/Re)^{12} + (K_1 + K_2)^{-3/2})^{1/12}$$

$$K_1 = [-2.457 \ln (7/Re)^{0.9} + 0.27 \ \epsilon_r/D_h]^{16} \tag{2.9}$$

$$K_2 = (37530/Re)^{16}$$

where ϵ_r is the wall absolute rugosity, and K_f is the loss factor, which is used for scaling the pressure loss to satisfy design specifications.

Then, the Equation 2.3 is computed with a centered strategy in a grid space, where ω, the conservation variables, and $\Omega(\omega)$, the source terms, will be evaluated in the center of every cell, that is, the nodes, and $f(\omega)$, the flux terms, at the interfaces, that is, the boundary between one cell and the next/previous one [2].

The components of ESPSS are classified in resistive or capacitive components, similar to the electrical circuits. A resistive component takes the state variables (density, pressure, enthalpy, chemical composition and velocity) as input data, and then calculate the flow variables, as volumetric, mass and enthalpy flows. The capacitive component makes the inverse process, so when the user is building a model up, he has to combine one resistive component with one capacitive, successively. The integral form of the Equation 2.3 is computed in a resistive component, for example a valve, as:

$$I_f(A\dot{G} + \dot{A}G) + I_v\dot{G} = \Delta p^o \begin{cases} 1 - \xi\frac{G|G|}{G_s^2} & (\frac{G_s}{G_c})^2 \leq \zeta \\ \\ 1 - \frac{G|G|}{G_c^2} & (\frac{G_s}{G_c})^2 > \zeta \end{cases} \qquad (2.10)$$

where G_s and G_c are the steady and critical mass fluxes, I_f and I_v represent the fluid and valve inertia and ζ the pressure loss coefficient, and the pressure drop can be expressed as:

$$\Delta p^o = (p + \frac{1}{2}\rho\nu^2)_{in} - (p + \frac{1}{2}\rho\nu^2)_{out} \qquad (2.11)$$

The steady solution to the upper branch for Equation 2.10 is $G = G_s\sqrt{\zeta}$, while for the bottom branch, the chocked conditions, it is $G = G_c$. The fluxes G_s and G_c can be computed as:

$$G_s = \sqrt{2\rho\Delta p^o}$$

$$G_c = \rho a \left(\frac{2 + (\gamma - 1)Ma^2}{\gamma + 1} \right)^{(\gamma+1)/2(\gamma-1)}$$

where the calculation of ρ, Ma and γ is calculated before entering in the valve. It is known that the pressure losses in the laminar range are proportional to the mass flow, so the source term can be linearized: $G|G| \rightarrow kG$ [**36 thesis victor**]. The pressure drop when there's turbulent flow, assuming constant area and a valve inertia close to zero, gives the family of solutions as

$$G(t) = \frac{G_s}{\sqrt{\zeta}}tanh\left(\frac{\Delta p^o\sqrt{\zeta}}{I_f AG_s}t\right) \qquad (2.12)$$

which solution is limited by the supercritical brand

$$G(t) = G_c tanh\left(\frac{\Delta p^o}{I_f AG_s}t\right) \qquad (2.13)$$

On its behalf, the capacitive components, volumes and mainfolds, solve the conservation equations of mass and energy:

$$\dot{\rho}V = \sum_{in}\dot{m}_{in} - \sum_{out}\dot{m}_{out} \qquad (2.14)$$

$$(\dot{\rho}e + \rho\dot{e})V = \sum_{in}(\dot{m}_{in}H)_{in} - \sum_{out}(\dot{m}_{out}H)_{out} \qquad (2.15)$$

As shown above, both resistive and capacitive components are employed together to solve the conservation equations that govern the problem. The resistive components are designed to solve the flow quantities $(\dot{m}, \dot{m}H)$, that are characterized by the flow area, whereas both the velocity and the state properties (h, T, ρ, p), are calculated by the capacitive components, characterized by its volume.

This document focuses on the thermodynamic modeling of air-breathing engines. Three different engines have been calculated; two of them in EcosimPro, the turbojet and the ramjet engine; and the Air Turbo-Rocket engine, ATR, which have been modeled in Matlab. The studies that have been made in the numerical software EcosimPro are exposed in Chapter 4.

3

The Air Turbo Rocket engine

3.1 Engine background

As commented previously, this document is totally focused in the modeling and study of the ATR engine. Designing a high-speed propulsion plant requires the compromise between the size of the engine, strictly linked with its weight, and the efficient utilization of fuel. As pointed below, the TBCCs have a very interesting feature that makes them good candidates to take part in the designing of the engine: their high specific impulse. The ATR engine is a particular case in which the turbine-based cycle is in charge of the acceleration stage of the trajectory, until a determined speed is reached, and the ramjet/scramjet module is able to be ignited. Thanks to this configuration, which combines components and characteristics from turbojets and rocket motors, the set of performances this engine offers is unique; high specific thrust and thrust-to-weight ratio over a wide operational range, talking about speed and altitude. These are the reasons why TBCCs constitute an excellent solution for these types of missions.
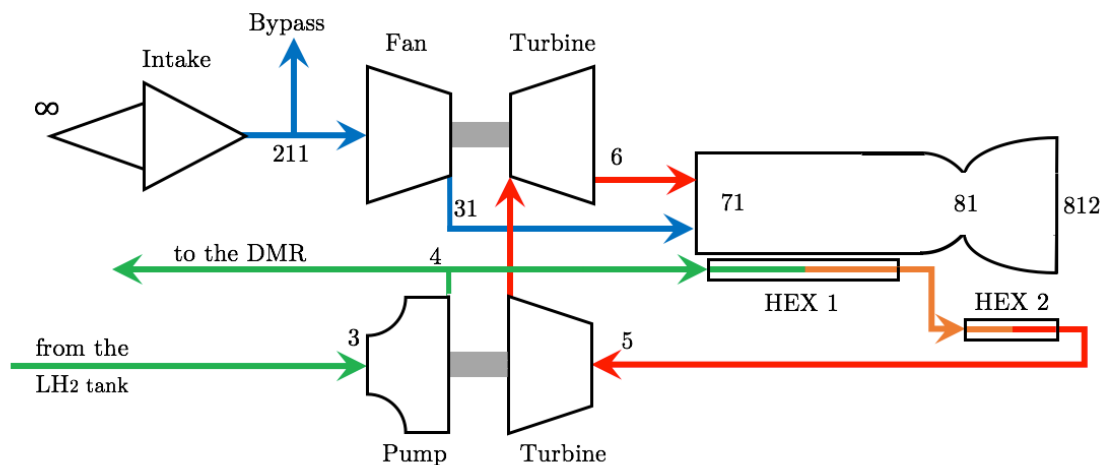

Figure 3.1: The ATR-EXP cycle

The Figure 3.1 shows the schematic representing the ATR-EXP cycle. There, it can be shown the flow path that both the air and the fuel (hydrogen) follow. First of all, the air is ram compressed in the intake, which is designed to work at a wide range of operation. From this station, it goes to the fan, that is driven by a generatively-heated fuel-powered turbine. Afterwards, the air advances to the preburner, in which is mixed and burned with the fuel. On its behalf, the fuel circuit is quite different. After going out of the tank, a pump leads the hydrogen to the heat exchangers, which constitute the regenerative cooling circuit for the burner and the nozzle. The heat pick-up is used to heat the fuel up, and then it goes through the turbine to the preburner, where it is mixed with the air, and straightaway burned. Then, the combustion gases enter in the final station of the circuit, the nozzle, to produce thrust and go out from the engine.

The ATR cycle presents some characteristics that make the engine one of the most powerful models for missions with wide ranges of operation: the shaft power delivered to the fan is independent from both the fan performance and the flight regime. Conversely, this feature is unsuitable talking about the engine stability if it is compared with the turbojet, since in this last cycle the fan and the turbine are coupled, so the surge or stall phenomenon is prevented by the own power delivered by the turbine [30]. As well, the altitude the ATR can reach is higher due to the higher combustion chamber pressure obtained, that is produced due to the combination of the fan work and the ram compression in the inlet. In addition, the turbine inlet temperature is no longer a limiting parameter which restricts the fuel injection and the flight speed, so the fan inlet temperature can be reached also when the compression in the intake reaches very high total temperatures due to the high velocity of the aircraft, and then this operational speed is increased by large compared with the turbojet [31]. Currently, the ATREX engine investigation is totally focused on the application to the Mach 8 cruise aircraft MR2 [6].

Figure 3.2: MR2 aircraft

The ATR developing had its first steps in the decade of 1960, when some patents started to come out [31]. Apart from the works of Luidens and Weber [13], in 1992 Lardellier and Thetiot [32] patented an ATR-GG combined to a ramjet. Later, in 1995, Bussi et al. [14] calculated the operating lines over the characteristic map of a two counter-rotating stages fan with variable pitch [33] at various flight conditions. Four years later, Christensen [31] made a research about the design and performance of an ATR working with a solid fuel gas generator. The turbomachinery employed for that study was specifically designed, and so were the maps.

Currently, the majority of the existing literature makes reference to the air turbo-rocket engine with gas generator. In terms of the expander type, ATREX is a pre-cooled ATR created in the 1980s, thought as a fly-back booster to accelerate a reusable TSTO space plane to Mach 6. For that mission, liquid hydrogen was employed to cool down the air stream that circulated through the inlet, and then the burner walls. Originally, the model was thought to have a configuration in which the turbine was located very close to the fan in order to reduce weight and size of the engine. In fact, carbon composites were utilized as well for that purpose. Later on, a workability study was carried out for a

modified ATREX with a conventional aft-turbine [34]. A more recent study was focused on a subscaled precooled turbojet, just designed for ground and flight tests, in order to study the work and efficiency of the precooling circuit [35].

At this moment the ATR engine is thought to be used in the MR2 civil transport aircraft, in which it would act as the booster to accelerate the airplane up to Mach 4-4.5 for having good conditions for igniting the DMR engines. Namely, this transition is carried out at Mach 4.5 and 24 km of altitude. The propulsion unit consists on one ATREX and two DMR engines, installed in parallel in the airframe shown in the Figure 3.3.
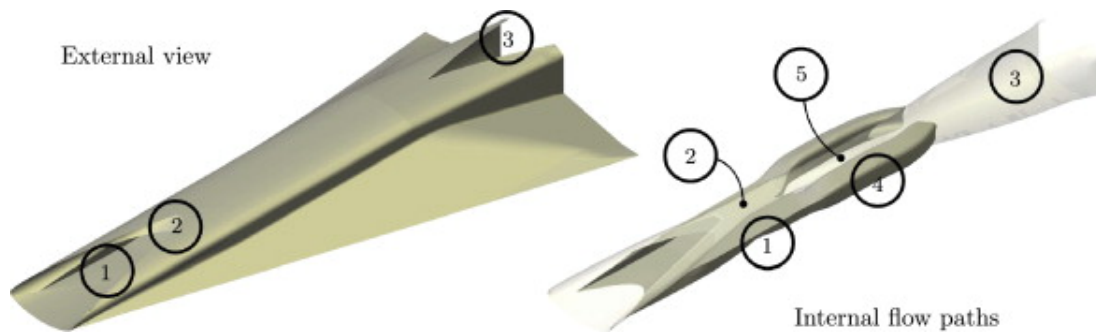

Figure 3.3: MR2, the civil transport aircraft. The numbers make reference to the stations: **1** low speed intake, **2** high speed intake, **3** nozzle, **4** ATR duct, **5** DMR duct. [2]

The air turbo-rocket engine has some significant parameters that, once identified, are the starting point to study the engine behavior in every point of its trajectory and working regime. As well, it is possible to carry out a parametric study and establish which are the optimum points where the turbine work is minimum and thus the engine size and weight, etc. Then, the following section is focused on identifying, analytically, which are the main parameters that will govern the system in the whole analysis.

3.2 Thermodynamic cycle

For the analytic study that is going to be carried out next, some assumptions have been taken in order to simplify the calculus and the formulation.

- The intake is assumed as ideal, so the TPR is equal to the unity.

- Both the air and the fuel are considered as perfect gases.

- The flow is analyzed in zero-dimensional conditions.

- Every component but the heat exchangers and the combustion chambers are assumed adiabatic.

- Steady regime is considered along the whole engine.

- The nozzle is adapted in all the trajectory.

- The liquid hydrogen that pass across the pump is considered as an incompressible flow.

To start the analysis, the specific work that is taken place in the turbine, pump and fan are expressed as

$$\Delta H_f = \frac{T_\infty^0 C_{pa}}{\eta_f} \left(\pi_f^{\frac{\gamma_a - 1}{\gamma_a}} - 1 \right) \tag{3.1}$$

$$\Delta H_p = \frac{(\pi_p - 1) p_3^0}{\eta_p \rho_3^0} \tag{3.2}$$

$$\Delta H_t = T_5^0 C_{ph} \ \eta_T \left(1 - \left(\frac{1}{\pi_t} \right)^{\frac{\gamma_h - 1}{\gamma_h}} \right) \tag{3.3}$$

where the subindexes f, p and t are referred to the fan, pump and turbine stations, respectively, and a and h to the air and the hydrogen flows.

Going on with the development, and taking into account that both the fan and the turbine discharge at the combustion chamber, it is possible to express the turbine expansion ratio, π_t, as a function of the pressure loss, δ_p, that takes place in the heat exchangers, the fan and pump compression ratios and the relation between fuel and the ambient pressures,

$$\delta_p = \frac{p_4^0 - p_5^0}{p_4^0} \tag{3.4}$$

$$\pi_t = (1 - \delta_p) \frac{\pi_p}{\pi_f} \frac{p_3^0}{p_\infty^0} \tag{3.5}$$

So, the Turbine Inlet Temperature, TIT, can be expressed as

$$T_5^0 = T_3^0 + \left(\frac{1}{\eta_p} - 1 \right) (\pi_p - 1) \frac{p_3^0}{C_h \rho_3^0} + \frac{q}{C_{ph}} MR \tag{3.6}$$

Notice that the second term of the expression at the right hand side makes reference to the temperature which is reached across the pump, and the third one is the increase of temperature that is produced when the flow goes through the heat exchangers. In addition, the reader can appreciate how the mixture ratio, MR, is influencing this heat addition, and this parameter can be written as

$$MR = \frac{\dot{m}_{31}}{\dot{m}_3} \tag{3.7}$$

If an energy balance across the shaft is applied, a power equilibrium is established between the turbomachinery of the engine.

$$MR \ \Delta H_f + \Delta H_p = \Delta H_T \tag{3.8}$$

The Equation 3.8 indicates that the turbine is driving both the fan and the pump. As it can be appreciated in the Figure 3.1, there are two turbines in the cycle, one driving the fan and one for the pump. Nevertheless, a single turbine is being consider. This is just for

analytic and modeling purposes, as it will be appreciated as well in the model developed in EcosimPro in the Chapter 5; one turbine can be considered to be responsible for the supply of the power which two of them would do in the reality.

Both the cycle behavior and performance, determined by the system composed by the equations 3.1 to 3.8, are modeled as a function of four parameters: the fan pressure ratio, the mixture ratio, the heat addition in the heat exchangers and the pressure loss throughout them.

$$\boldsymbol{Y} = f\left(\pi_f, MR, \frac{q}{C_{ph}T_3^0}, \delta_p\right) \tag{3.9}$$

As well, the following demonstration will prove that the performance of the engine is independent of the heat addition to the hydrogen flow, q, and the pressure drop that takes place in the heat exchangers, δ_p. It will be exposed that the performance parameters (specific thrust, specific impulse) and independent from these parameters, and thus from the engine size (nozzle area), and dependent just of the fan pressure ratio and the mixture ratio (for a given flight condition).

To start with, it is necessary to obtain the fan exhaust total temperature and total pressure,

$$T_{31}^0 = T_{21}^0 \left(1 + \frac{\pi^{\frac{\gamma-1}{\gamma}} - 1}{\eta_{cc}}\right) \tag{3.10}$$

$$P_c^0 = P_{21}^0 \pi_f \tag{3.11}$$

where P_{21}^0 is the total pressure at the inlet of the fan that, once gone through the intake, is the ambient total pressure multiplied by the inlet total pressure recovery,

$$P_{21}^0 = P_0^0 \ TPR \tag{3.12}$$

Now, it is possible to obtain the chamber total temperature that is reached when the combustion takes place,

$$T_c^0 = \frac{MR \ C_p \ T_{31}^0 + \eta_{cc}L}{(1 + MR)C_p} \tag{3.13}$$

The nozzle is always adapted, so it is imposed that the nozzle area ratio is changing constantly while the trajectory is being followed, satisfying the design condition in which $P_9 = P_{amb}$. As a result, the exhaust velocity of the engine can be expressed as

$$V_n = \sqrt{\frac{2\gamma R_\gamma T_c^0}{\gamma - 1}\left(1 - \left(\frac{p_{amb}}{p_c^o}\right)^{\frac{\gamma-1}{\gamma}}\right)} \tag{3.14}$$

So V_n is function of p_c^o and mixture ratio. The net thrust is calculated by Eq. 3.15, which expresses that, for a given flight condition and fuel and air massflow, it is function of the nozzle exhaust velocity and nozzle efficiency.

$$T_N = m_a \left[\left(1 + \frac{1}{MR} \right) V_n \eta_n - V_0 \right] \tag{3.15}$$

The specific thrust, then, can be obtained from

$$T_{sp} = \left(1 + \frac{1}{MR} \right) V_n \eta_n - V_0 \tag{3.16}$$

Efficiencies, specific impulse and specific fuel consumption are obtained from the following expressions.

$$\eta_o = \frac{T_N V_0}{\dot{m}_{H_2} H_p} = \frac{MR \left[\left(1 + \frac{1}{MR} \right) V_n \eta_n - V_0 \right] V_0}{H_p} = \frac{MR T_{sp} V_0}{H_p} \tag{3.17}$$

$$\eta_p = \frac{2 T_N V_0}{\dot{m}_{th} V_n^2 - \dot{m}_a V_0^2} = \frac{2 \left[\left(1 + \frac{1}{MR} \right) V_n \eta_n - V_0 \right] V_0}{\left(1 + \frac{1}{MR} \right) V_n^2 \eta_n - V_0^2} \tag{3.18}$$

$$\eta_{th} = \frac{\dot{m}_{th} V_n^2 - \dot{m}_a V_0^2}{2 \dot{m}_{H_2} H_p} = \frac{MR \left[\left(1 + \frac{1}{MR} \right) V_n^2 \eta_n - V_0^2 \right]}{2 H_p} \tag{3.19}$$

$$\eta_o = \eta_{th} \eta p \tag{3.20}$$

$$I_{sp} = \frac{T_N}{\dot{m}_{H_2} g} = \frac{\eta_o H_p}{g V_0} = \frac{T_{sp} MR}{g} \tag{3.21}$$

$$TSFC = \frac{\dot{m}_{H_2}}{T_N} = \frac{V_0}{\eta_o H_p} \tag{3.22}$$

As a conclusion, it can be state that the performance parameters can be calculated independently of the size, and then re-scaled (A_{th}) to satisfy the necessity of the mission.

3.3 Operational functioning for a given mission

As stated in section 3.1, the MR2 follows a trajectory clearly defined, in which not only the flight condition (altitude and flight velocity) is already planned, but also the installed thrust, $\mathcal{F}$, that is required to make the mission possible [2]. Figures 3.4 and 3.5 show both the mission trajectory and the installed thrust.

As well, Figures 3.6 and 3.7 show the intake total pressure recovery along the flight Mach number, and the air massflow ratio between the total massflow that enters in the engine and the one that goes through the ATR engine, calculated by [36]. It is necessary to mention that the engine is composed by two modules, ATR and DMR ones, and both of them share the first intake. Then, there is a control surface that controls whether the ATR intake is opened or not, as well as the DMR one, and logically it depends of the flight condition. The section designed for the ATR is called LSI, Low Speed Intake, and the one for the DMR, HSI, High Speed Intake. Both capture ratios are calculated as

$$\alpha_c^{LSI} = \dot{m}_{21}/\dot{m}_0$$

$$\alpha_c^{HSI} = \dot{m}_{20}/\dot{m}_0$$

where $\dot{m}_{21}$, $\dot{m}_{20}$ and $\dot{m}_0$ are the air massflows going into the ATR module, DMR module and main intake for both ones, respectively.
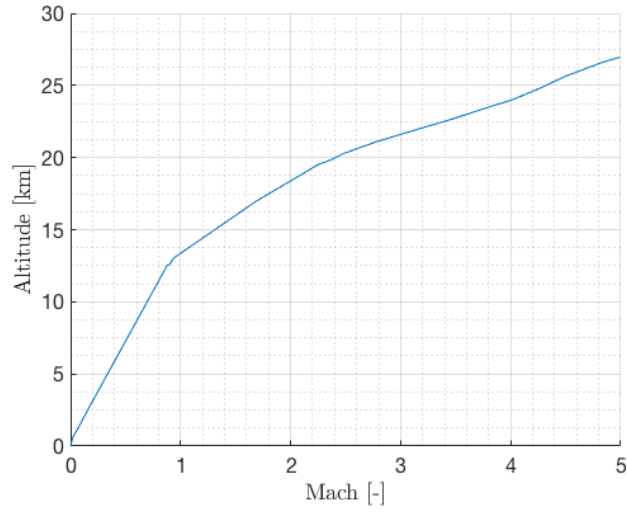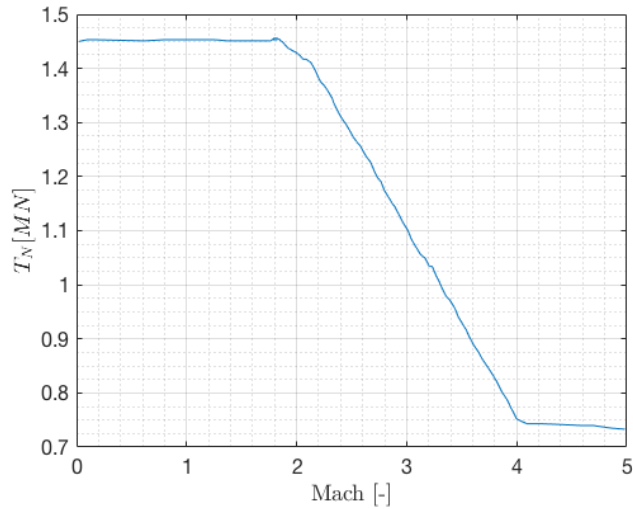
Figure 3.4: MR2 trajectory

Figure 3.5: MR2 installed thrust

For a mission in which the installed thrust is given, and taking into account that the specific thrust is already obtained, the air massflow needed for the intake is calculated in Eq. 3.23,
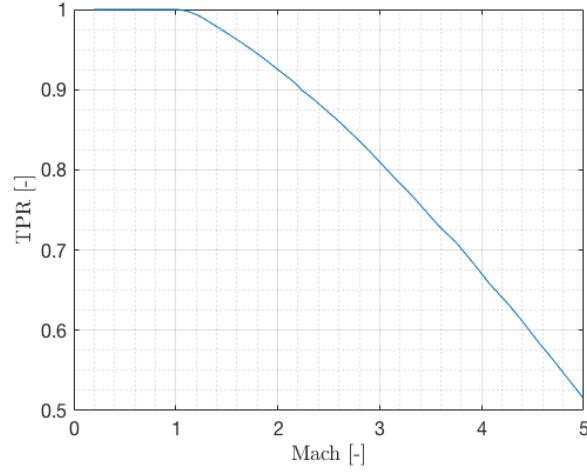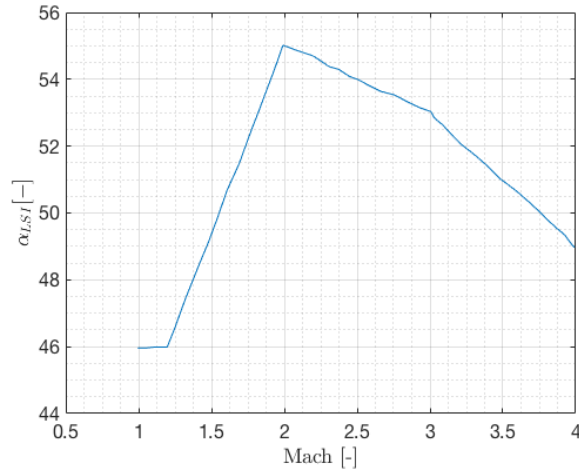
Figure 3.6: MR2 intake TPR

Figure 3.7: MR2 Low Speed Intake ratio

$$T_{sp} = \frac{\mathcal{F}}{\dot{m}_{21}} \tag{3.23}$$

For the supersonic regime, and depending on the working point, there is a limit in which the air massflow that goes through the LSI is higher than $\dot{m}_{21}$. As a result, some bleeding is necessary to respect the design condition. Consequently, a minimum T_{sp} is defined,

$$T_{sp} \geqslant \frac{\mathcal{F}}{(\rho\nu)_{\infty} \ A_0 \ \alpha_c^{LSI}} \tag{3.24}$$

where $(\rho\nu)_{\infty} \ A_0 \ \alpha_c^{LSI}$ is the air massflow that enters in the ATR intake, $\dot{m}_{21}$. Taking into account this restriction, a bleeding ratio is defined as,

$$B = \frac{\dot{m}_{bypass}}{(\rho v)_\infty \ A_0 \ \alpha_c^{LSI}} = \frac{\dot{m}_{bypass}}{\dot{m}_{21}} \tag{3.25}$$

So the bleeding ratio, which is as well a quantification of the excess of thrust if no bleeding is applied, can be expressed also as a function of the specific thrust,

$$B = 1 - \frac{\mathcal{F}}{(\rho v)_\infty \ A_0 \ \alpha_c^{LSI} \ T_{sp}} = 1 - \frac{T_{sp}^{min}}{T_{sp}} \tag{3.26}$$

where the T_{sp}^{min} corresponds to the limit value established by Eq. 3.24.

The minimum nozzle area is calculated differently for both the subsonic and the supersonic regime. For both regimes, the nozzle area is function of V_n, MR and the conditions in the combustion chamber, and in the supersonic one, there is also one more parameter; the bleeding ratio. The area in subsonic conditions is obtained from Eq. 3.27, and the one for supersonic conditions, from Eq. 3.28.

$$A_9 = \dot{m}_{21} \left(1 + \frac{1}{MR}\right) \frac{R_c T_9}{P_9 V_n} \tag{3.27}$$

$$A_9 = (\rho v)_\infty \ A_0 \ \alpha_c^{LSI}(1 - B) \left(1 + \frac{1}{MR}\right) \frac{R_c T_9}{P_9 V_n} \tag{3.28}$$

being P_9 the pressure at the exhaust of the nozzle, equal to P_{amb}, due to the nozzle is considered as adapted.

$$T_9 = T_c^0 \left(1 - \eta_n \left(1 - \left(\frac{P_9}{P_c^0}\right)^{\frac{\gamma-1}{\gamma}}\right)\right) \tag{3.29}$$

For the throat area calculation, the following procedure is followed:

$$P_{crit} = P_c^0 \left(1 - \frac{1}{\eta_n} \frac{\gamma-1}{\gamma-1}\right)^{\frac{\gamma}{\gamma-1}} \tag{3.30}$$

$$P_{th}^0 = P_{crit} \left(1 + \frac{\gamma-1}{2} M_{th}^2\right)^{\frac{\gamma}{\gamma-1}} \tag{3.31}$$

$$M_9 = \frac{V_n}{\sqrt{\gamma \ R \ T_9}} \tag{3.32}$$

$$P_9^0 = P_9 \left(1 + \frac{\gamma-1}{2} M_9^2\right)^{\frac{\gamma}{\gamma-1}} \tag{3.33}$$

$$\frac{A_9}{A_{th}} = \frac{P_{th}^0}{P_9^0} \frac{1}{M_9} \left(\frac{2}{\gamma+1}\left(1 + \frac{\gamma-1}{2} M_9^2\right)\right)^{\frac{\gamma+1}{2(\gamma-1)}} \tag{3.34}$$

Finally, the turbine power is calculated from the specific turbine work, which is independent from the engine size, Eq. 3.3.

$$\dot{W}_t = \begin{cases} \Delta H_t \ \dot{m}_{21}/MR & Ma_\infty < 1 \\ \Delta H_t \ (\rho v)_\infty \ A_0 \ \alpha_c^{LSI}(1 - B)/MR & Ma_\infty \geqslant 1 \end{cases} \tag{3.35}$$

Once shown the whole procedure to compute and calculate the cycle that models the ATR-EXP behavior, several studies have been carried out, and results are going to be proposed in the Chapter 5. The studies that have been made are:

- Influence study of each meaningful parameter over the cycle.

- Operational range of the engine, focusing on the turbomachinery cycle, varying its meaningful parameters to study the work made by the turbine and the ones consumed by the pump and the fan.

- Performance (Tsp and Isp) of the calculated operational range.

- Minimum throat area needed for the correct functioning of the engine versus the fan pressure ratio, and showing it in function of MR, bleed and turbine work.

- Turbine work versus fan pressure ratio.

Engine modeling in EcosimPro

4.1 Turbojet engine

In this section, an easy example of using EcosimPro is going to be carried out, in order to show the way to proceed in this software. First, a schematic of the engine is going to be introduced in the Figure 4.1, as well as the stations numbering.
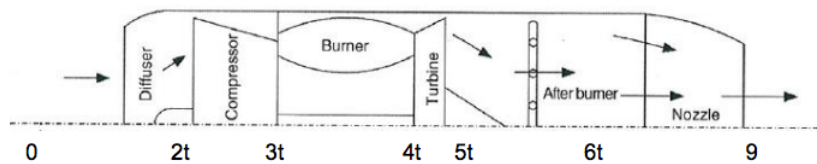

Figure 4.1: Schematic of the turbojet engine

Then, the model has to be created by choosing the components and connecting them. For that purpose, the library TURBOJET is going to be used. There, all the components needed for this type of engine can be found. So, it is necessary to select and drag the components to the workspace and connect them by means of their ports.
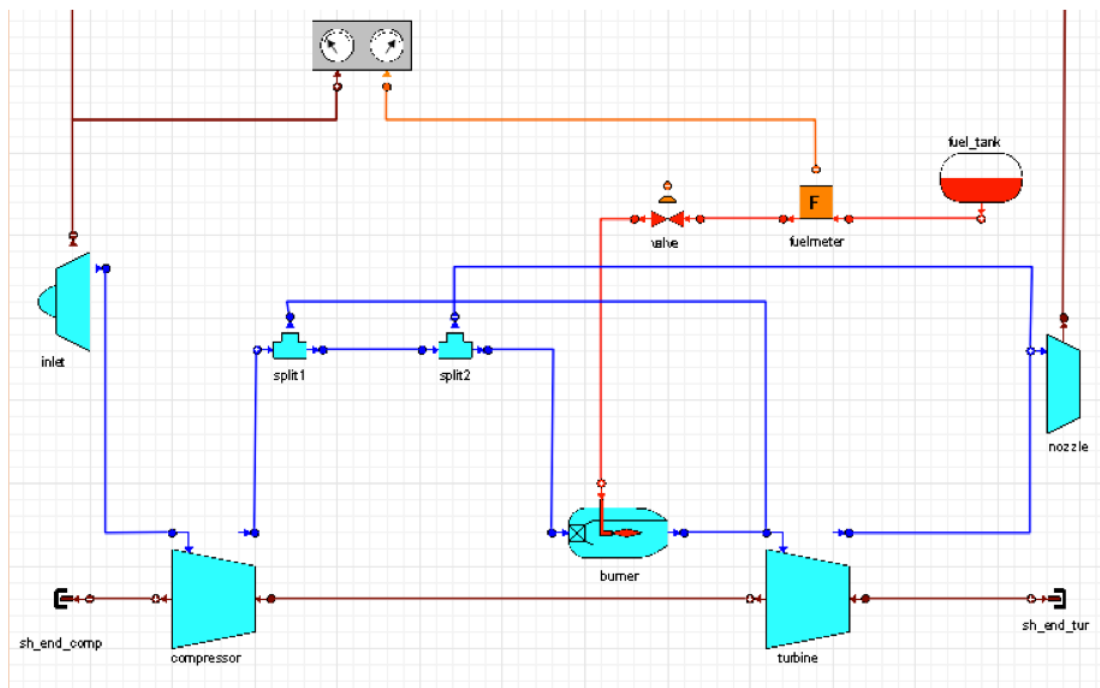

Figure 4.2: Turbojet engine model in EcosimPro

Figure 4.2 shows that the engine is composed by eleven types of components. First, the intake receives the air and decelerates it to discharge the flow to the compressor. Then, there are two splits that are modeled as the cooling circuit that is going to be discharged in the turbine and in the nozzle. If the air is going in its natural path, it will be driven to

the combustion chamber, where will be mixed with the fuel. Notice that there is a valve controlling the fuel flow that enters in the burner, by means of a law that is coming from a monitor located in the upper part of the workspace. After the burner, the turbine and nozzle stations take place, and there the model is closed and finished.

The points that are next to the components represent the ports, and there is the start or the end of the line that connects one component with the following one. Notice that there are different lines depending on its color, which represents the type of port they are linked to. The blue ones are referred to the fluid type, and it is understood as the flow circulation throughout the components. The brown one represents the mechanical type. In this model, it is representing the shaft that connects the compressor with the turbine. On its behalf, the red line is representing the flow circulation. In general, this is not happening in other libraries, but only in the TURBOJET one. In the others, all flows are represented by fluid type ports, but in this library it seems that the air and the fuel are differentiated. The orange one corresponds to the control library, which is in charge of establishing all the control laws that governs the engine behavior. With this laws, the user could choose to change, for example, the beta parameter of the compressor in function of the entering mass flow, or the nozzle area in function of the fuel massflow added to the burner. Finally, the other brown line, which is going from the inlet to the nozzle is a nozzle type, which is for monitoring the thrust generated by this last component. Naturally, there are more types of ports, but their explanation exceeds the goals of this document if they are not included in the model utilized here.

Going on with the turbojet modeling procedure, the next step is to create the partition; the mathematical model defining the tearing variables, the initial and boundary conditions, the unknown data and the algebraic variables. This is one of the most critical steps when modeling a system with EcosimPro, due to the fact that the user cannot define a system he wants if the variables chosen are not correct, that is, that do not close the system of equations. This procedure can be done by default by EcosimPro, which will choose the mathematical model and create the partition automatically, or by the user, for whose procedure some wizards will be used. The Figure 4.3 shows one of the wizards used to create the partition. Namely, it is the one focused on choosing the boundary conditions, which is the critical step. The followed procedure to create the partition is the following one:

- Select the unknown variables of the problem. If this step is skipped out, the mathematical model could assume a value for variables that, in other way, should be unknowns. In the first phase of designing, there are variables that are totally unknowns and need to be defined for subsequent calculus, such as the geometry (pipe and valve areas, length of the ducts, etc.), the nominal speed of the moving parts of the engine, the initial mass flow or the pressure rise of pumps.

- Remove dynamic variables from the equation system by deriving some equations, if it is possible. This is due to that some dynamic variables depend on other dynamic variables and thus cannot be integrated independently, so it is logical to think that this step is not always needed.

- Establish the boundary conditions. This step is not only deciding which are going to be the external conditions of the engine (temperature, pressure, velocity...) but also
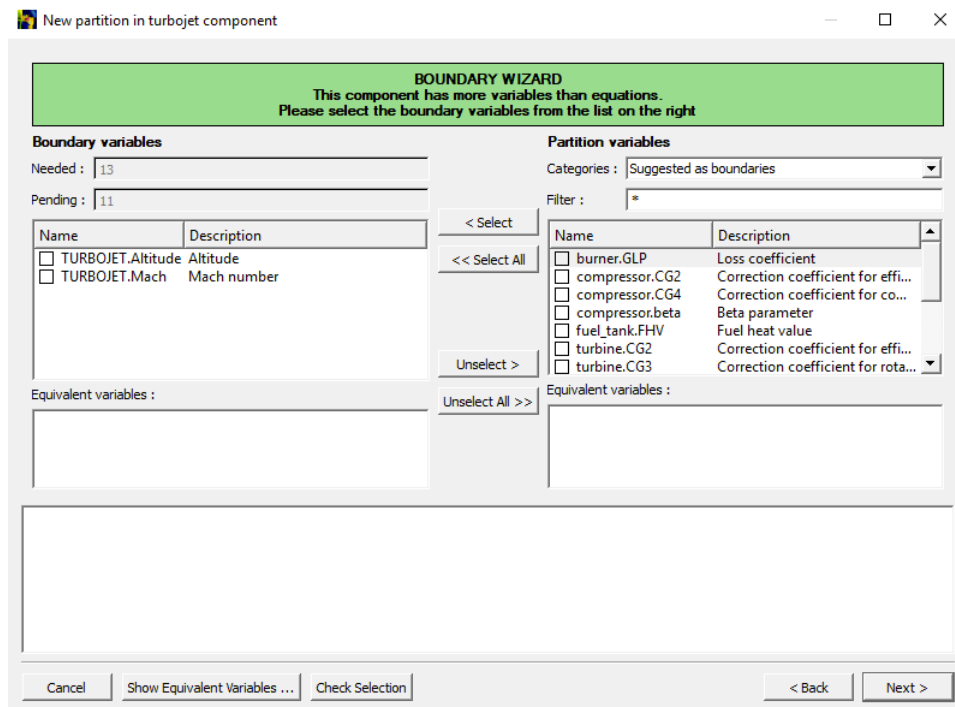
Figure 4.3: Boundary conditions wizard to create a partition in EcosimPro

the variables that the user do know. For instance, in the turbojet model, studying its stationary behavior, the user could specify the compressor pressure ratio and the efficiency of all the components as known variables.

- The last step is the algebraic wizard. When a non-linear algebraic equation system is detected, the wizard assists the user to select the minimum set of algebraic variables to solve the non algebraic box. EcosimPro is going to suggest a set of algebraic variables, but of course is the user the one who chooses the final set. Nevertheless, the software checks that selection and validates it or generates an error, asking a change of variables to close the system correctly (physically speaking).

Finally, the partition is created, so does the mathematical model. In this stage of the process, the experiment is going to be created, which constitutes the final step before running the calculus and analyze results. As commented before, the experiment is the tool needed to establish the numerical values to the algebraic variables, the boundary conditions and other variables whose default value could be modified. For doing all these tasks, the experiment is divided in several blocks, where the code is organized by categories in function of their function in the code:

- The DECLS block is used to store and declare all the variables utilized in the experiment. If the user is going to calculate a mass flow and name it as $\dot{m}$, then he has to declare it in this block, specifying its type, which in this case will be REAL. As described above, there are lots of types, such as TABLE1D, STRING, INTEGER, BOOLEAN, etc.

- The OBJECT block is employed to use instances of C++ classes.

- The INIT block is designed for initialize dynamic and algebraic variables whose derivatives appear in the formulation, as well as the algebraic unknowns. However, this block is only needed for the variables that are not previously initialized, not for all of them. An important feature of the system is that the dynamic variables are fixed in the problem, but not the algebraic unknowns. The model could contain implicit equations, so the number of algebraic variables that are treated in this block has to be equal to the number of implicit equations. As well, it is important to establish a coherent numeric value for the variables, due to the fact that the closer the number is to the solution, the less time the simulation takes. Moreover, if the values are so far from the final ones, results could converge into an unreal solution.

- The BOUNDS block is the one which sets the expressions for the boundaries of the model. They can be not only numerical values, but also expressions depending on time. During the experiment, the user can modify any boundary variable, and the software will detect by its own when it is needed to reinitialize and modify these variables.

- The last block is called BODY. The difference with other blocks is that this is used for several tasks, not just one, like integrate models, calculate steady states, generate reports, etc. In this unit, the integration time is selected, the integration step, the absolute and relative error, the solver used (Runge-Kutta, DASSL adn DASSL-SPARSE), and hundreds of other tasks.

Following the turbojet example, and providing the engine with correct input data, which some of them are indicated in the Table 4.1, it is possible to calculate the cycle and make an study of its behavior. First, the cycle will be analyzed choosing a single point, and comparing its data with other software, GasTurb. Results are shown in Table 4.2

Parameter	Value	Units
Flight altitude	4000	M
M_0	1.5	-
$\dot{m}_a$	70	$kg\ s^{-1}$
Burner Air Loading	2.5	$kg\ s^{-1}\ m^3$
π_{cc}	0.99	-
π_c	12	-
Compressor β parameter	0.7	-
η_T	0.9	-
TIT	1300	K

Table 4.1: Input data for the turbojet calculus

Once the design point is calculated, it is time to study the influence of one or several parameters in the engine performance. As this is being done just for illustrative purposes, no conclusions related to the thermodynamic cycle are going to be obtained from these results.

Parameter	EcosimPro value	GasTurb value	Units
T_2	380.1	379.9	K
P_2	2.24	2.26	bar
T_3	798.4	784.9	K
P_3	26.9	27.2	bar
T_4	1300	1300	K
P_4	26.6	26.9	bar
T_5	936.1	947.7	K
P_5	5.9	6.1	bar
Nozzle outlet Ts	800.6	784.9	K
Net Thrust	29.02	29.64	kN
$\dot{m}_f$	1.02	1.02	$kg\ s^{-1}$
FAR	0.0146	0.0146	-
TSFC	35.18	34.43	$g\ kN^{-1}s^{-1}$
A_{exit}	0.093	0.090	m^2
η_o	0.4	0.37	-

Table 4.2: Design point calculated in EcosimPro and GasTurb

For the current study, a single parameter has been selected to be changing in the cycle; the Turbine Inlet Temperature, TIT. As mentioned before, there is no interest in the thermodynamic cycle of the engine, so just two parameters are going to be shown, in order to compare and validate the model of both programs. These parameters will be the nozzle throat area and the gross thrust. First, gross thrust will be showed for both programs, and then the nozzle area.
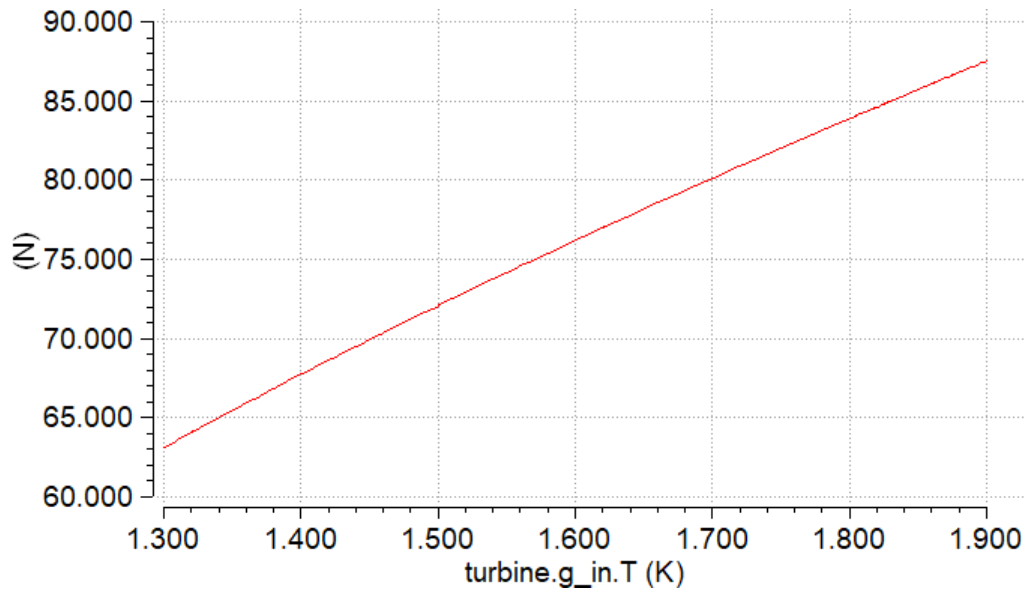
Figure 4.4: Thrust vs TIT for a turbojet engine, modeled in EcosimPro
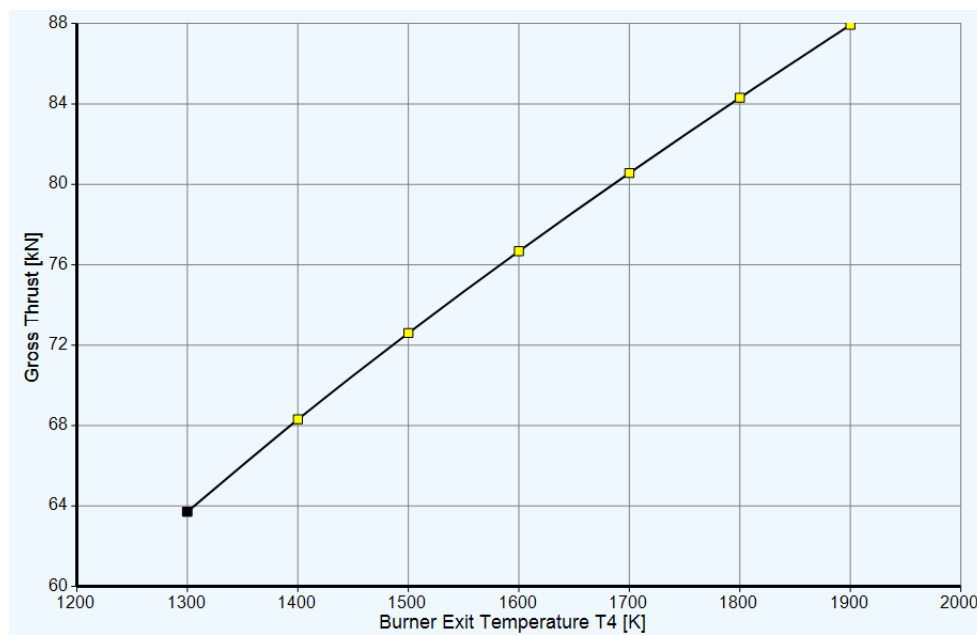
Figure 4.5: Thrust vs TIT for a turbojet engine, modeled in GasTurb
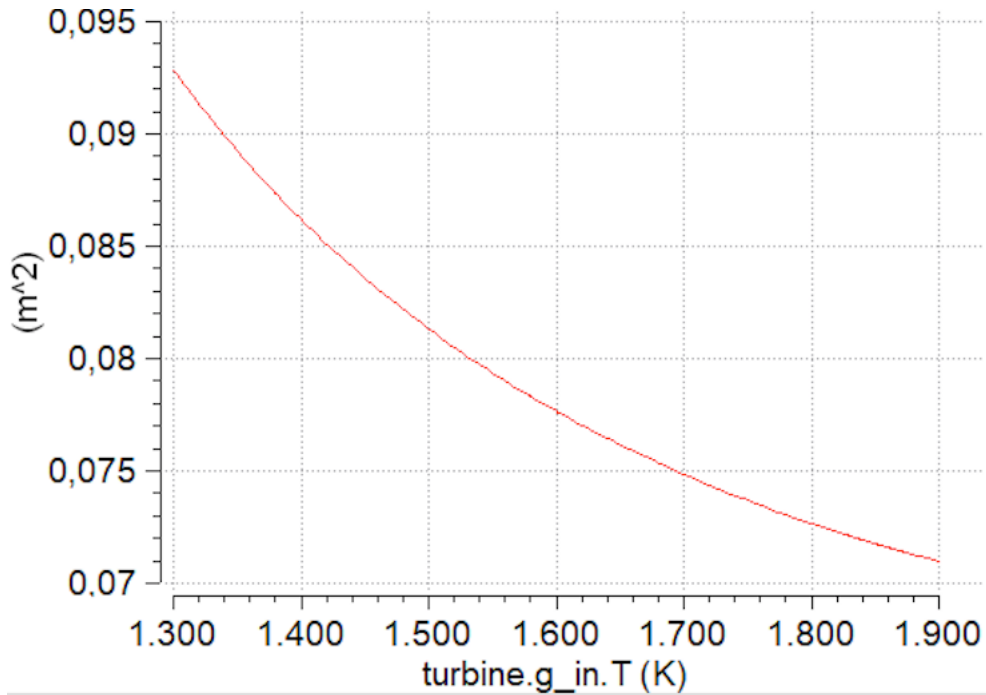
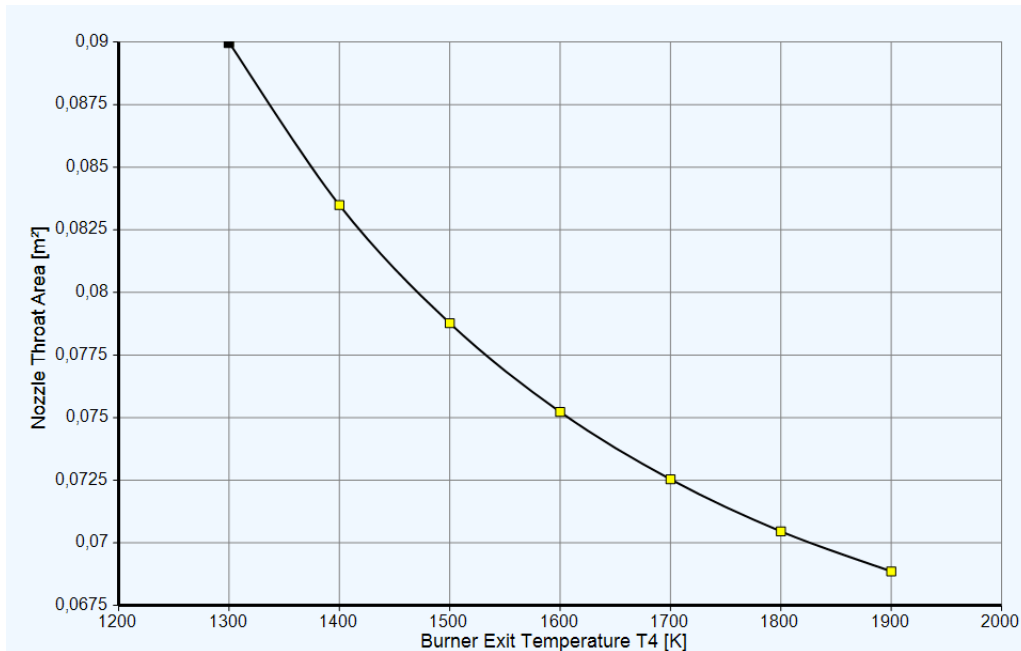Figure 4.6: Nozzle area vs TIT for a turbojet engine, modeled in EcosimPro

Figure 4.7: Nozzle area vs TIT for a turbojet engine, modeled in GasTurb

The reader can appreciate that results extracted from both programs are quite similar. The discrepancies shown in Table 4.2 and in the exposed Figures are related to the different models GasTurb and EcosimPro use for calculating the cycle. EcosimPro is a

more complex software that takes into account processes that are not present in GasTurb, such as losses in pipes, in valves, more complete chemical interactions resolution, etc. Nevertheless, both models present similar results, so the one that the user has done in EcosimPro can be cataloged as validated.

4.2 Ramjet engine

In this section, a ramjet cycle model is going to be introduced. There will be two studies which will be presented. The first one consists on a design point calculus, in which the boundary conditions (flight altitude and Mach) will be imposed. The second one will calculate all the operational points included in a huge range of altitude and Mach. In the first stage of the problem, the schematic which contains the model has to be defined in EcosimPro, which can be observed in Figure 4.8.
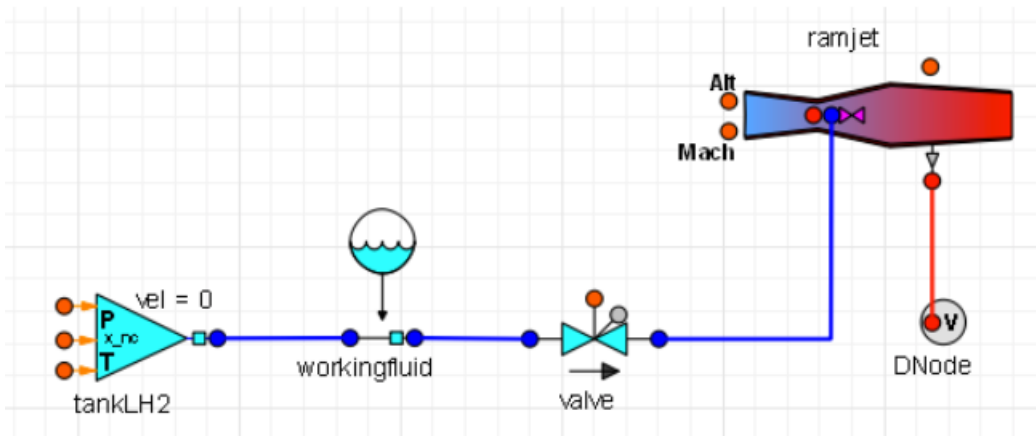
Figure 4.8: Ramjet schematic in EcosimPro

As Figure 4.8 shows, the ramjet engine is composed by a single component that models the whole behavior of the engine. It actuates as a "black box" in which the user introduces certain input parameters and obtain the appropriate results. If the user desires to know the functioning of this black box, he has to consult the code directly, as it has been done in this document to understand the functioning of valves, thrust calculation, pressure losses in injectors, etc. Apart from the ramjet component, the schematic counts with a valve that can regulate the fuel massflow entering in the engine. The orange point that appears in the component is a control port, so a control law can be assigned to the valve to set the amount of flow going through the valve, according to certain parameters such as altitude or flight velocity.

4.2.1 Single point calculus

This study is focused in the calculus of a single point of the trajectory, in which some input parameters are going to be introduced and then an analysis of the engine behavior will be performed. Then, using the schematic presented in Figure 4.8, a partition and an experiment is created, following the same procedure than the one indicated in Section 4.1.

Parameter	Value	Units
Altitude	8000	m
Flight Mach	5	-
η_{cc}	0.98	-

Table 4.3: Initial parameters for a single point calculus in the ramjet engine

Table 4.3 shows some relevant parameters. However, some others must be indicated, such as the combustor starter temperature, the pressure the H2 (the fuel used in this calculus) tank will have, or the length of the ramjet, but there is no need to detail them in the document because this study is centered in a qualitative analysis, not quantitative. Moreover, this section will not cover a steady calculus of the ramjet cycle. Instead, an experiment in which the fuel valve and the burner igniter are switched off and suddenly connected on will be made. The signal related to the valve, employed to this purpose, is shown in Figure 2.
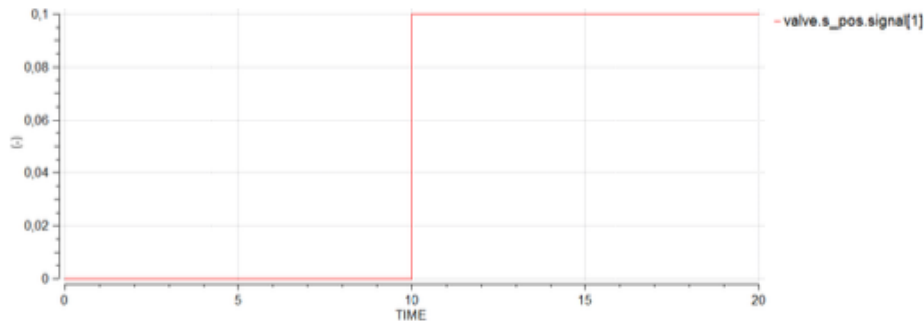
Figure 4.9: Valve position vs time

As it has been modeled, the valve will let the fuel flow go into the core when the simulation is at the instant TIME = 10 s. Nevertheless, the combustion will start when TIME = 15 s, due to the fact that the igniter will be activated at this instant. This type of inputs brings the possibility to study the engine behavior before and after the fuel is added. Then, the results are presented in Figures 3 to 6. In addition, this technique helps the numerical model gain some stability and velocity at the beginning of the calculus, rather than initialize all the variables at the same time.

Once the boundary variables have been established, running the model is the next step. Figures 4.10 to 4.13 show the results obtained in this study.
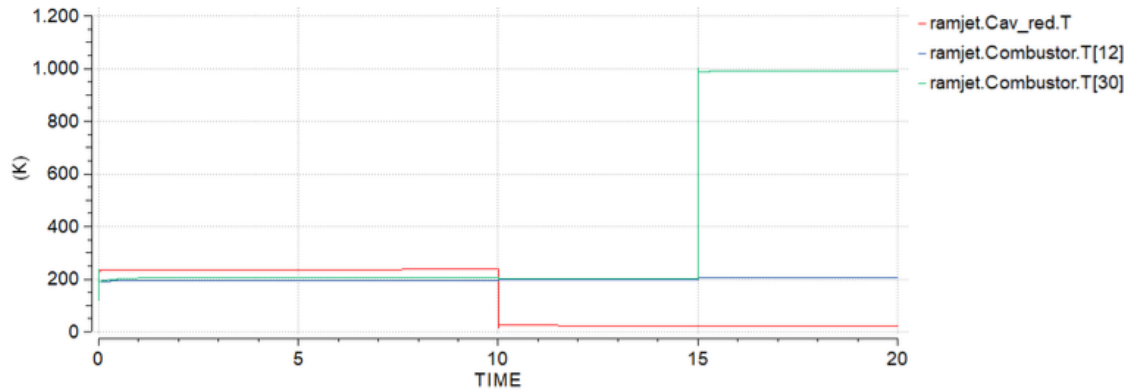
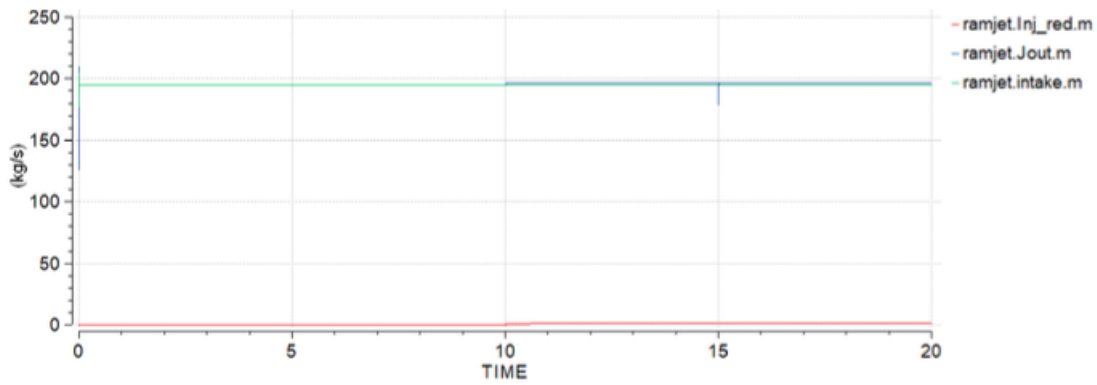Figure 4.10: Temperatures at nodes 1, 12 and 30 in the ramjet combustion chamber

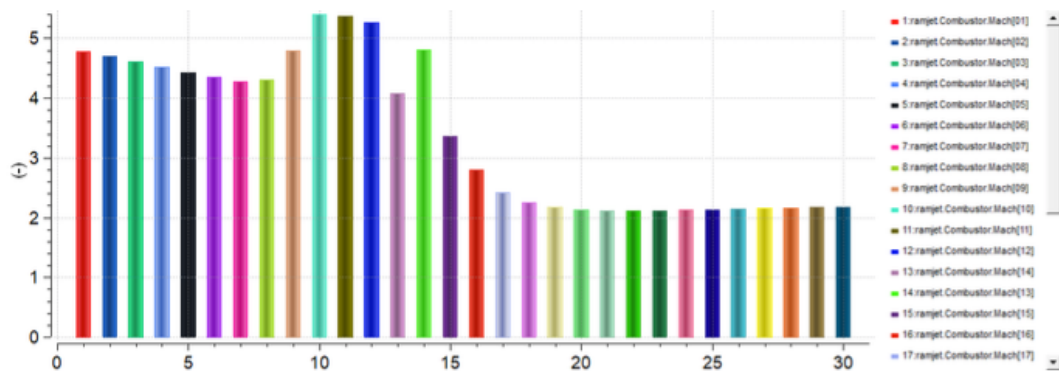Figure 4.11: Air, fuel and total massflows

Figure 4.12: Mach number histogram inside the combustion chamber

As the results show, the influence of the fuel flow addition and the igniter activation can be easily noticed looking at the previous figures. Figure 4.10 shows the temperature that some nodes of the combustion chamber reach. This chamber is discretized in 30 nodes to guarantee some accuracy. A prove of the total freedom that EcosimPro offers the user to model thermodynamic processes such as combustion is the possibility to choose where
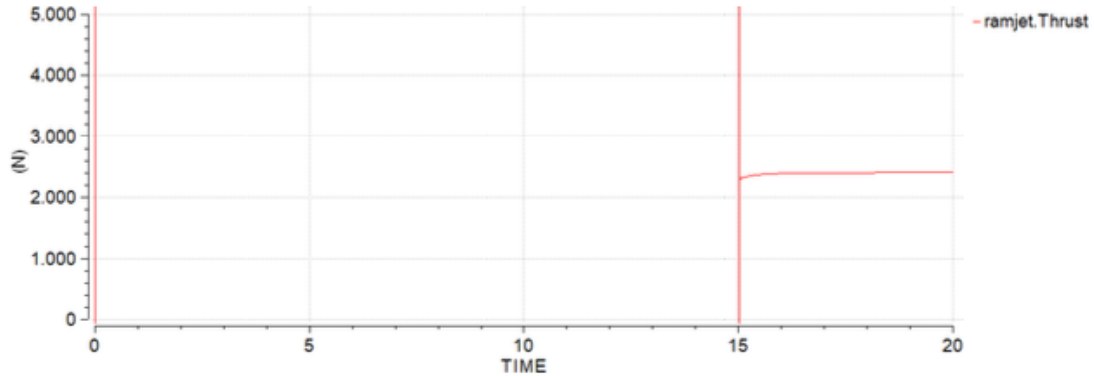
Figure 4.13: Ramjet engine thrust

the fuel is going to be injected. In this example, the fuel is introduced in the chamber in the nodes 20 to 24, 20 % each node, so as the results indicate, just the nodes above the twentieth are going to increase its temperature. According to this, the node 30 is the only one that increment its temperature in this graph. On its behalf, the massflow shown in Figure 4.11 is increased in TIME = 10s, due to the valve opening.

As Figure 4.12 indicates, EcosimPro allows the user to plot histograms of variables along the chamber discretized in nodes. This is very useful to examine how a variable is evolving across both the time and the length. In this case, the Mach number is computed, having its maximum at node 9, and reaching stability around the twentieth node.

Finally, thrust is shown in Figure 4.13. As it shows, there is a huge instability in the beginning, reaching negative values due to the fact that there is no fuel injection nor ignition. When this last phenomenon takes place, stability is reached and the software is able to converge in a reasonable value, which is the final result of the experiment.

4.2.2 Parametric study

In a second phase of the ramjet analysis, a parametric study will be performed in order to observe the influence of the flight conditions, as well as the operational range of the engine. Therefore, a wide interval has been selected, both for altitude and flight Mach, as it is shown in Table 4.4.

Parameter	Interval	Step	Units
Altitude	2000 - 20.000	2000	m
Flight Mach	3 - 6	0.1	-

Table 4.4: Boundary conditions for the parametric study

Then, the results are introduced in the Figures 4.14, 4.15 and 4.16. Clearly, there is a range of operation for each altitude and Mach. Regarding fuel-to-air ratio, FAR, and temperature, there exist a value of this two variables for almost every operational point, despite of the fact that there are many illogical values, such as extremely low burner ex-

haust temperatures or high fuel-to-air ratio values, so that is because there are some parts of the lines that are "dashed"; because these illogical values are NaN values in the matrixes.

Analyzing the tendencies of the variables exposed, the FAR is increasing with the altitude because the fuel massflow is determined by the difference of pressure between the fuel tank and the combustion chamber. While the tank pressure is constant, the combustion chamber one is decreasing with altitude, so there is an increasing pressure gradient, which motivates the entering of larges amount of H_2 fuel in the chamber. Nevertheless, the Mach number makes the FAR decreases when it increases. That is because the amount of air massflow that enters in the engine is higher, so the proportion makes the FAR lower. Regarding the temperature in the combustion chamber, it is clear that the more fuel injected, the more temperature is increased, reaching its maximum in the stoichiometric value. That is why the temperature follows a similar tendency than the FAR. On its behalf, the thrust is following similar tendencies than the other ones, establishing a clear operational range for values of temperature and velocity. If the FAR could be maintained constant, the thrust could maybe increase due to the increase of air massflow when the Mach number is increased, and as well being increased (the thrust) when the altitude is higher, due to the lower air density. Nevertheless, as the fuel-to-air ratio is decreasing and so is the chamber temperature, so it motivates a decrease in the nozzle exhaust velocity, and consequently in the net thrust the engine produces.
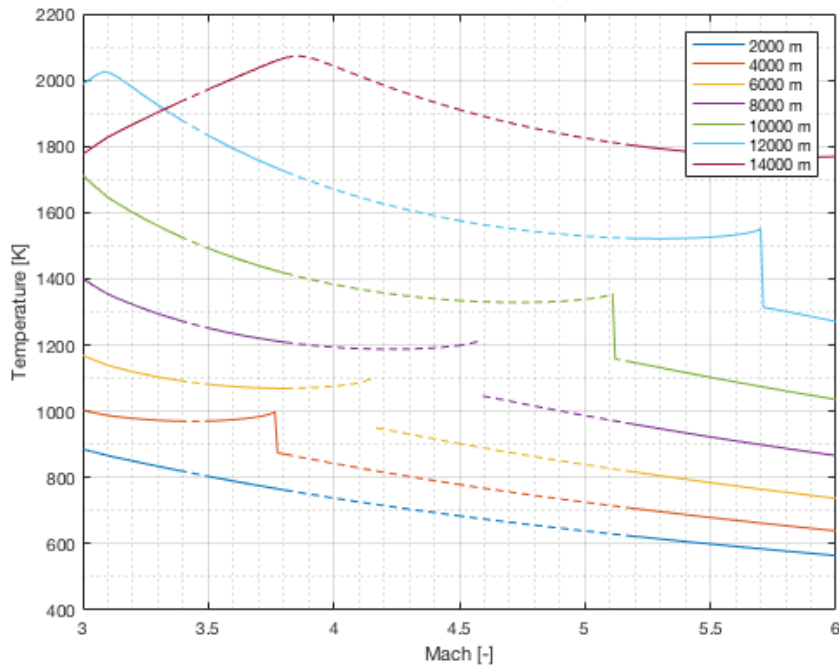

Figure 4.14: Combustion chamber temperature vs altitude and Mach number
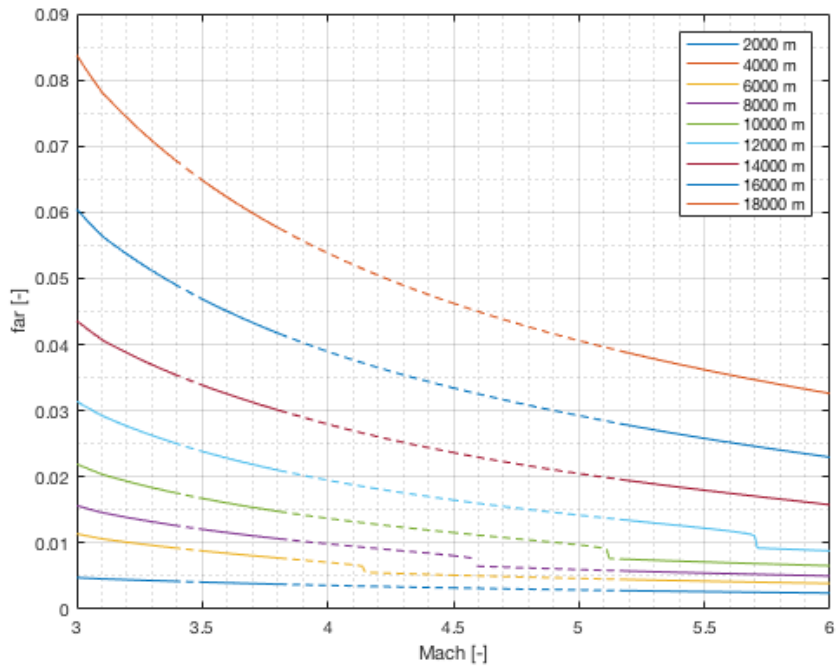
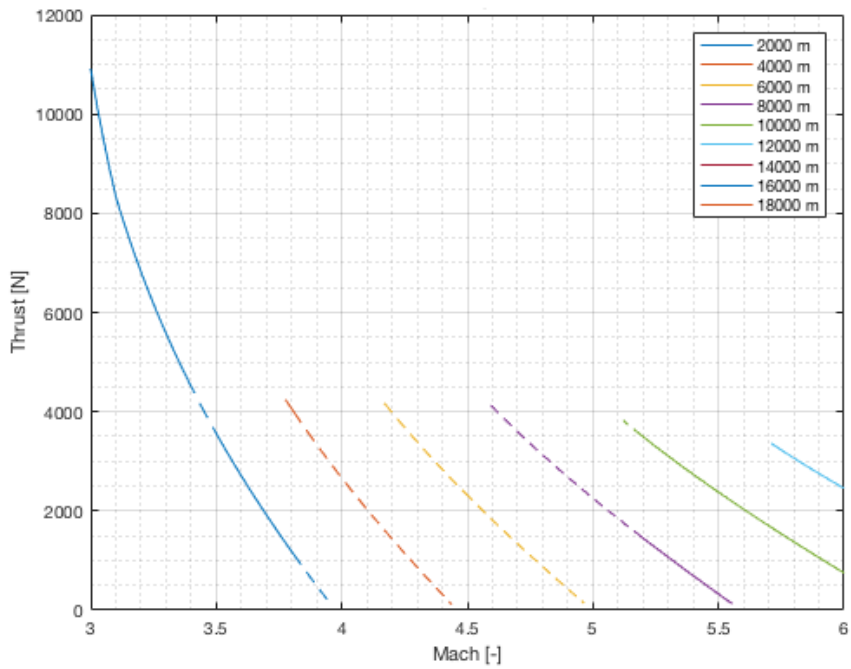Figure 4.15: Fuel-to-air ratio vs altitude and Mach number

Figure 4.16: Ramjet engine thrust vs altitude and Mach number

4.3 High-speed propulsion engines modeling

In this document, the ATR engine has been studied analytically in Matlab, but it has been developed as well in EcosimPro. The schematic of the engine has been created, and the partition development and the configuration of experiments is proposed for future works.
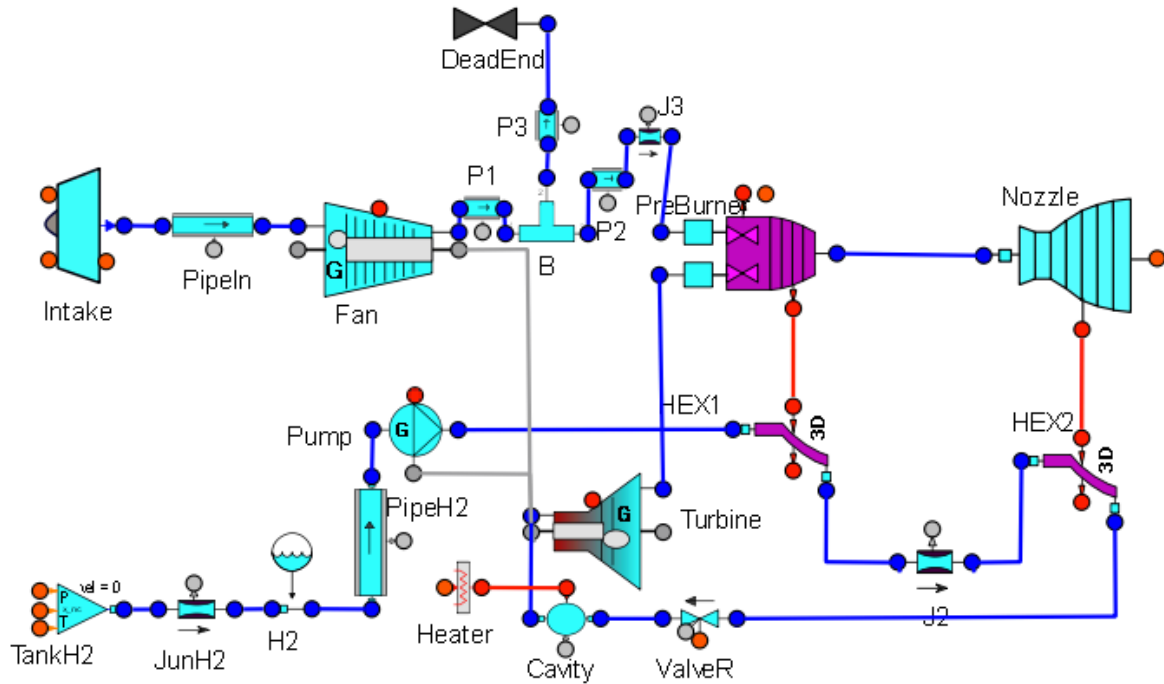

Figure 4.17: Air Turbo-Rocket Expander engine schematic in EcosimPro

Figure 4.17 represents the schematic that is going to be used for the ATR cycle modeling. It follows the same structure than the Figure 3.1 There, it can be shown the flow path that both the air and the fuel (hydrogen) follow. First of all, the air is ram compressed in the intake, which is designed to work at a wide range of operation. From this station, it goes to the fan, that is driven by a generatively-heated fuel-powered turbine. Afterwards, the air advances to the preburner, in which is mixed and burned with the fuel. On its behalf, the fuel circuit is quite different. After going out of the tank, a pump leads the hydrogen to the heat exchangers, which constitute the regenerative cooling circuit for the burner and the nozzle. The heat pick-up is used to heat the fuel up, and then it goes through the turbine to the preburner, where it is mixed with the air, and straightaway burned. Then, the combustion gases enter in the final station of the circuit, the nozzle, to produce thrust and go out from the engine.

This schematic has some particularities that need to be commented. First, the bleeding is modeled by a Tee-component that conducts part of the air out of the engine, and it is necessary not to have an excess of air in the supersonic regime. Second, notice that there is a Heater that models the heat exchange that the cooling jackets components, named as HEX1 and HEX2, extract of both the PreBurner and the Nozzle to heat up the H_2

massflow. Finally, a single turbine is used for driving both the pump and the fan, just for simplifying purposes in the modeling task.

The ATR schematic has been introduced in this document. As stated before, the partition development and the configuration of experiments are proposed as future tasks, in order to compare them with the analytic studies that are going to be exposed in the next chapter.

5
Studies and Results

This chapter is focused on showing the different studies that have been made on the ATR engine, which have been introduced in the Chapter 3, and its discussion and analysis. It is necessary to remark that these studies have been carried out analytically in Matlab. The studies that have been made are:

- Influence study of each meaningful parameter over the cycle.

- Operational range of the engine, focusing on the turbomachinery cycle, varying its meaningful parameters to study the work made by the turbine and the ones consumed by the pump and the fan.

- Performance (Tsp and Isp) of the calculated operational range.

- Minimum throat area needed for the correct functioning of the engine versus the fan pressure ratio, and showing it as a function of MR, bleed and turbine work.

- Turbine work versus fan pressure ratio. and mixture ratio.

5.1   Influence study

As there are four meaningful parameters of the ATR cycle, it is interesting to know the sensitivity of each of these parameters in the general behavior of the engine. Consequently, an influence study has been made: first of all, a reference case has been calculated, whose meaningful parameters values are exposed in Table 5.1.

Variable	Value	Units
π_f	2.5	[-]
MR	35	[-]
$\dot{q}$	500	[kJ/kg]
δ_p	0.1	[-]

Table 5.1: Input data for the meaningful parameters of the thermodinamic cycle

Then, four studies in which one parameter varied its value a 10% have been made.That is the reason why Table 5.2 have five columns: the first one shows the results of the reference case, and the following ones are referred to the four studies performed. There, the specific works of the turbomachinery have been specified, as well as its variation with the reference case. As well, this procedure has been followed for the performance parameters.

As the Table 5.2 shows, the parameters that have more influence over the cycle are the π_f and the MR. Logically, the π_f is the only parameter that affects to the fan specific work, Eq. 3.1. As well, it has a strong influence in the turbomachinery performance, so this is one of the most important meaningful parameters to study. On its behalf, the mixture ratio has less importance in the turbomachinery work, but it is important in the performance parameters. It can be shown that the π_f and the MR are the only ones that

Cases/Variables	Reference	$\Delta\pi_f$	ΔMR	Δq	$\Delta\delta_p$
ΔH_f value [kJ]	166.2	144.8	166.2	166.2	166.2
ΔH_f variation [%]	-	12.87	0	0	0
ΔH_p value [kJ]	814.7	331.8	765.2	465.7	835.1
ΔH_p variation [%]	-	59.3	6.1	42.83	2.5
ΔH_t value [kJ]	6621.3	5389.6	7153.6	6272.4	6641.7
ΔH_t variation [%]	-	18.6	8.03	5.27	0.3
T_{sp} value [kJ]	1.57	1.54	1.48	1.57	1.57
T_{sp} variation [%]	-	1.6	5.9	0	0
I_{sp} value [kJ]	55.1	54.2	57	55.1	55.1
T_{sp} value [%]	-	1.6	3.5	0	0

Table 5.2: Influence study over the turbomachinery cycle

affect to the specific thrust and specific impulse, as it was stated in Chapter 3.2. The heat addition is a parameter that strongly affects to the turbine and the pump. As the heat is added to the fuel, it only affects to its cycle, so that is the reason why this parameter has no influence neither to the fan specific work nor to the performance parameters. Finally, the pressure drop on the heat exchangers is the last parameter to analyze. As it is exposed in the table, just a 2.5 % of variation in the pump specific work takes place when varying a 10% the value of the δ_p. So, it is correct to state that this variable has much less importance over the thermodynamic cycle than the other ones.

As a result of this study, the following ones are going to be developed by varying the fan compression ratio, the mixture ratio, and the heat addition. The pressure drop is not going to be part of the parametric study due to its little influence over the thermodynamic cycle.

5.2 Operational range of the engine

This study is focused on finding a combination of the meaningful parameters to get to achieve the establishment of the operational line along the trajectory of the MR2 while the ATR engine is working. As the trajectory may be discretized in thousands of points, and this is an analytical and qualitative study in which the computational cost would be extremely high to be performed in Matlab, just several points will be calculated, and they are shown in Table 5.3.

	1	2	3	4	5	6
M_0 [-]	1.1	1.7	2.1	3.2	4	4.5
h [km]	13.9	17	18.9	22	24	25.6

Table 5.3: Trajectory points used for the operational range study

Then, the study consists on varying the value of the π_f, the mixture ratio and the heat extracted from the preburner and nozzle by the heat exchangers to add it to the fuel flow,

and compare it with the turbine expansion ratio, π_t, that would be necessary to drive both fan and pump under those conditions. As well, the pump and turbine specific work divided by the mixture ratio vs the heat addition is going to be shown to expose the clear influence of this parameter with the turbomachinery performance.

To start with, the study related with the first point, $M_0 = 1.1$ and h = 13.9 km will be exposed. The Figure 5.1 shows the turbine expansion ratio vs the heat addition, with three different fan pressure ratios and a range of mixture ratio from 20 to 50.
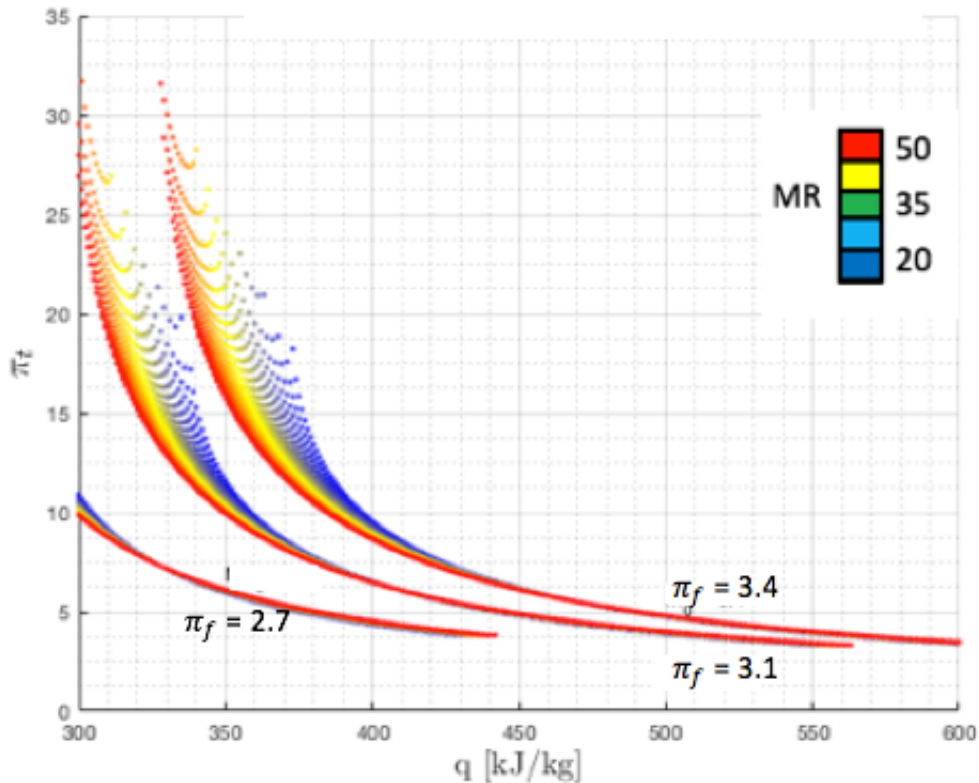
Figure 5.1: Turbine expansion ratio vs heat addition to the working fluid, at $M_0 = 1.1$

As it is exposed in Figure 5.1, the higher the π_f, the more heat addition is necessary to decrease the π_t. It has to be taken into account that the purpose of adding heat to the fuel is decreasing the turbine pressure ratio (downsize the turbine) so the engine size is lower, and thus the weight. The mixture ratio does not influence very much the turbine expansion ratio, and just in the range from 300 to 400 kJ its influence is noticeable: when the fuel massflow is decreased (more mixture ratio) the turbine inlet temperature increases, so it compensates the decrements of the fuel flow rate that is going through the turbine, considering constant π_t.

As it can be observed in this figure, there is a trade-off between the heat extracted by the heat exchangers and the turbine expansion ratio: the attempt to develop a cycle with low turbine expansion ratio is conditioned by the amount of heat that the heat exchangers are able to extract. As stated before, it would be the optimum condition, in order to

reduce size and weight. Nevertheless, doing a big turbine would make possible to operate without such an efficient and powerful heat exchanger.

In the end, what it is intended is to increase both specific thrust and specific impulse, so this study is focused on choosing the correct combination of parameters, but trying to accomplish this condition. This analysis will be analyzed deeply in the Section 5.3.

Continuing with the results exposition, the specific works vs the heat addition to the fuel is going to be exposed.
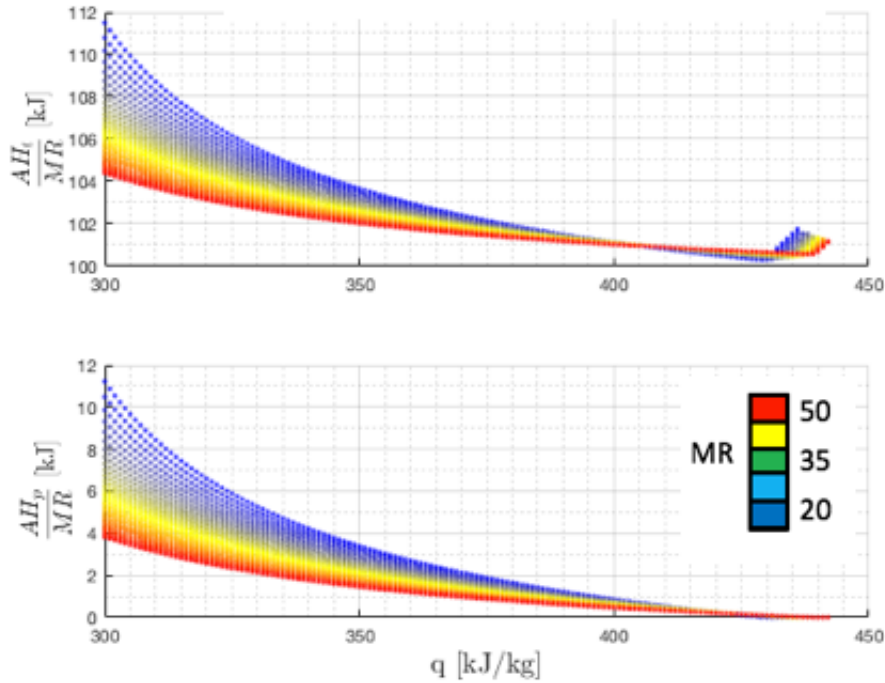
Figure 5.2: Turbine and pump specific work vs heat addition to the working fluid, at $M_0 = 1.1$ and $\pi_f = 2.4$

Paying attention to Figures 5.2, 5.3 and 5.4, it can be observed that both the pump and turbine specific works are decreasing with the increase of heat addition. That is predictable, taking into account the turbine expansion ratio in the Figure 5.1, and the Eqs. 3.2 and 3.3, where it is shown that the pump work is proportional to the turbine one. As well, it is noticeable that the pump power is two orders of magnitude lower than the turbine one, so this is the cause why the engine performance is insensitive to the pressure loss in the heat exchangers and the pump.

Talking about the engine behavior when the π_f is increased, it is shown that the specific work on the turbine and the pump has to be higher. On its behalf, the mixture ratio is influencing the works in a narrow range of heat addition, just similar to the Figure 5.1.
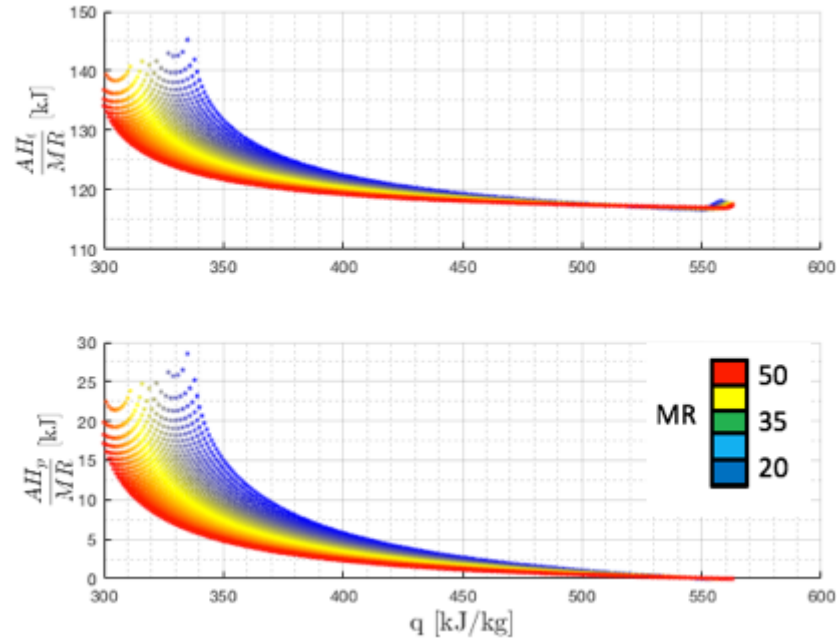
Figure 5.3: Turbine and pump specific work vs heat addition to the working fluid, at $M_0 = 1.1$ and $\pi_f = 3.1$
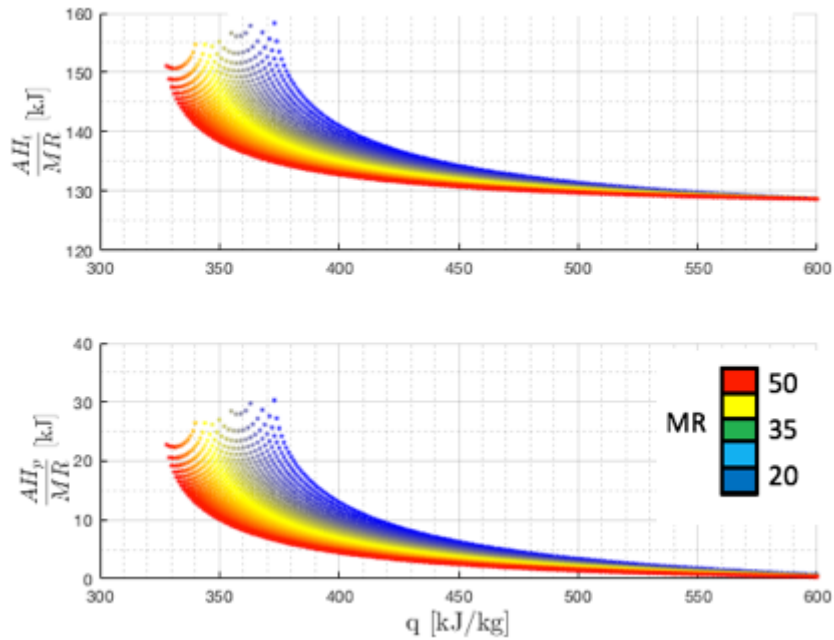

Figure 5.4: Turbine and pump specific work vs heat addition to the working fluid, at $M_0 = 1.1$ and $\pi_f = 3.4$

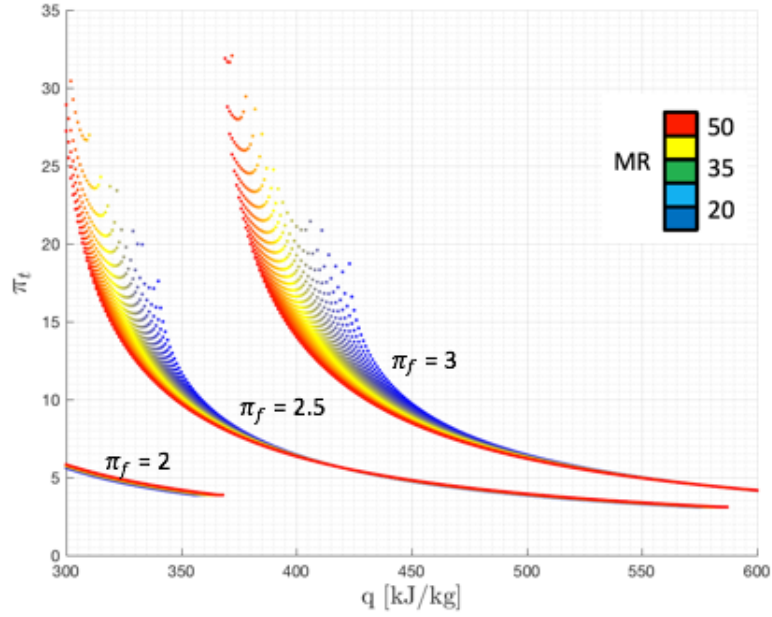Now, results from the point 2, $M_0 = 1.7$ and h = 17 km are going to be shown.

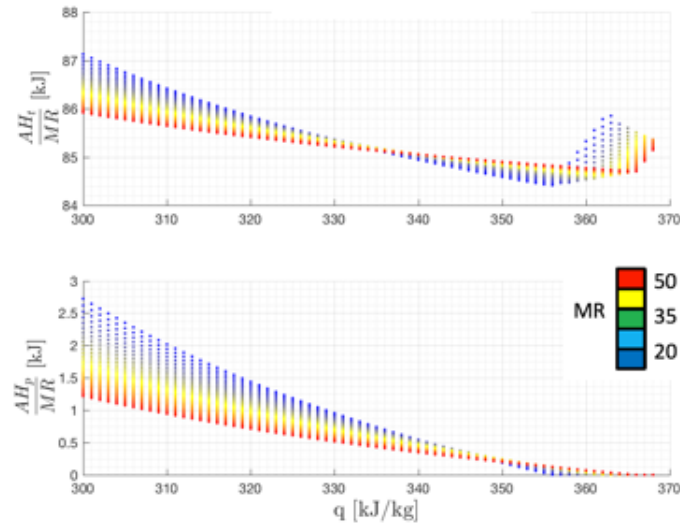Figure 5.5: Turbine expansion ratio vs heat addition to the working fluid, at $M_0 = 1.7$

Figure 5.6: Turbine and pump specific work vs heat addition to the working fluid, at $M_0 = 1.7$ and $\pi_f = 2$

Showing the results from the point 2, $M_0 = 1.7$ and h = 17 km, it is clear that the tendency is quite similar, but with some particularities. Comparing Figures 5.1 and 5.5, it is clear that the more velocity the engine is flying at, the more influence has the fan pressure ratio. It can be observed that there is a higher separation between curves in 5.5 than in the previous one. Then, it means that the more π_f needed, the more π_t has to be overcome. On its behalf, the heat addition is very important to low down the turbine expansion ratio, so at these velocities this parameter is even more important than before.

Separately, the mixture ratio has some influence at low heat addition, when the more fuel flow in the mixture, the more heat the engine needs, in order to be able to make a good combustion process.
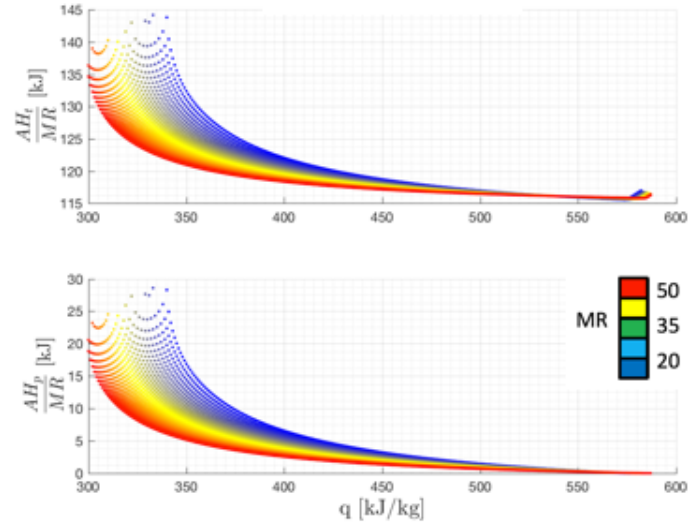

Figure 5.7: Turbine and pump specific work vs heat addition to the working fluid, at $M_0 = 1.7$ and $\pi_f = 2.5$
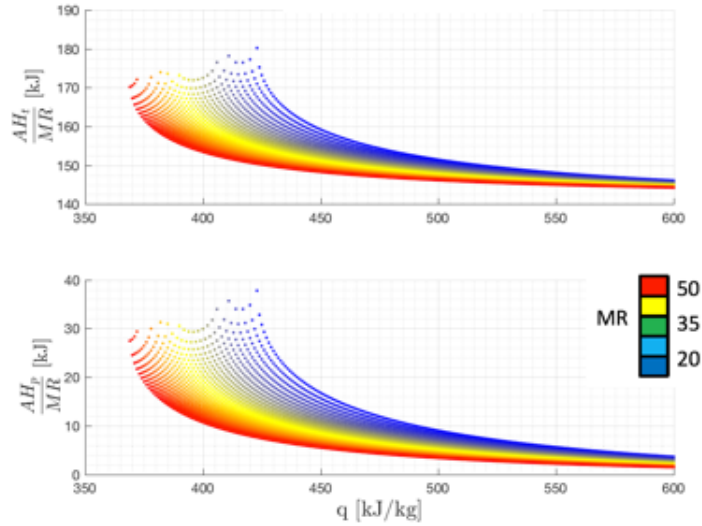

Figure 5.8: Turbine and pump specific work vs heat addition to the working fluid, at $M_0 = 1.7$ and $\pi_f = 3$

Figures 5.6, 5.7 and 5.8 show both the pump and the turbine specific works divided by the mixture ratio, vs the heat addition. It can be noticed that the engine power demand is maximum between this regime and the previous one, $M_0 = 1.7$. The maximum levels

of specific power take place along these two points, so they establish the maximum power that the turbine has to provide as a design constraint.

Now, results from the point 3, $M_0 = 2.1$ and h = 18.9 km are going to be shown.
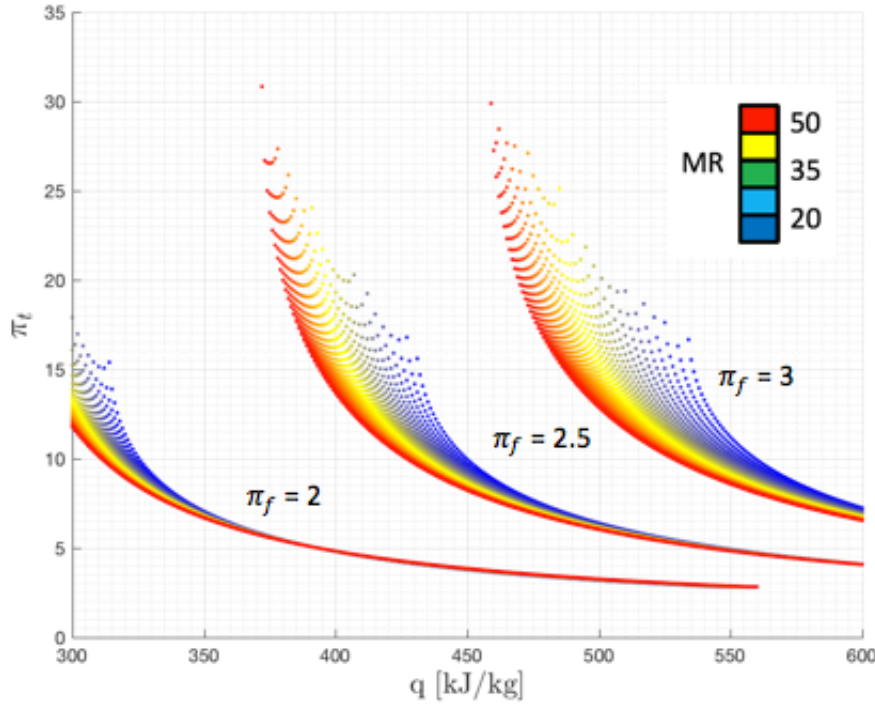

Figure 5.9: Turbine expansion ratio vs heat addition to the working fluid, at $M_0 = 2.1$

Figure 5.9 shows the turbine expansion ratio the engine needs at this flight condition. Following the tendency of the previous flight regimes, it can be observed that the fan compression ratio affects considerably to the π_t demanding. The curves are more separated than the previous regimes, so operating with $\pi_f = 3$ would be logical if there were a heat exchanger capable of providing such amount of heat. If that is not the case, the turbine expansion ratio would have to be extremely high to satisfy this operation, so it is better off to operate at low fan compression ratios to decrease the turbine size and weight, and have less heat demand from the heat exchangers.

Figures 5.10, 5.11 and 5.12 follow an interesting tendency that needs to be commented. The power demand of the engine at this flight condition is close to the maximum that the cycle is going to need along the whole trajectory. That means that this area is the critical one, talking about design terms. Then, analyzing the specific works, it is noticeable that the curves admit just a certain range of heat addition to operate with, so here it is clear the importance of the heat addition. Not only a big turbine would be needed, but also a heat exchanger that is able to provide the enough amount of heat to satisfy the cycle demand. If there is no heat exchanger, there is no cycle, as it is observed in the ranges of 300 to 370 in the Figure 5.11. There are no values there because there exists an extremely high value of turbine expansion ratio, impossible to achieve in the reality, but possibly

as a mathematical solution of the general system of equations. The mixture ratio is an important parameter under this flight condition, in which it can be observed that there is a big difference of heat needed for the same turbine expansion ratio when changing the MR from 20 to 50. This is clear in Figure 5.12.
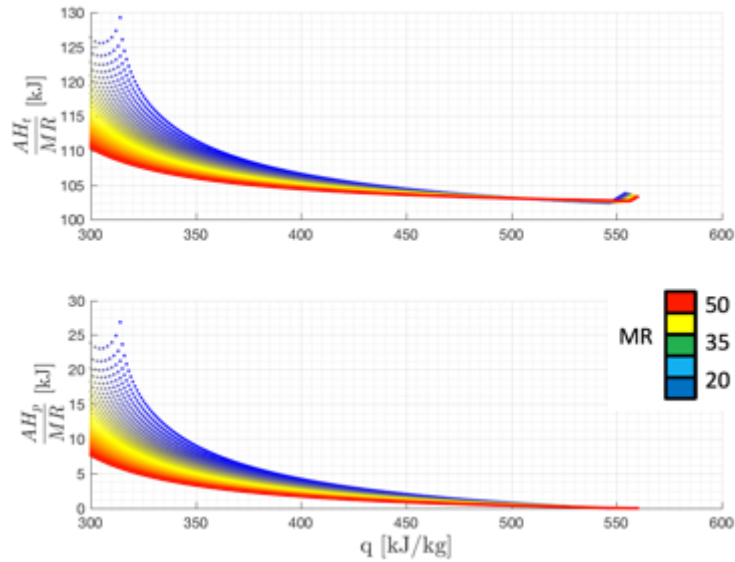

Figure 5.10: Turbine and pump specific work vs heat addition to the working fluid, at $M_0 = 2.1$ and $\pi_f = 2$
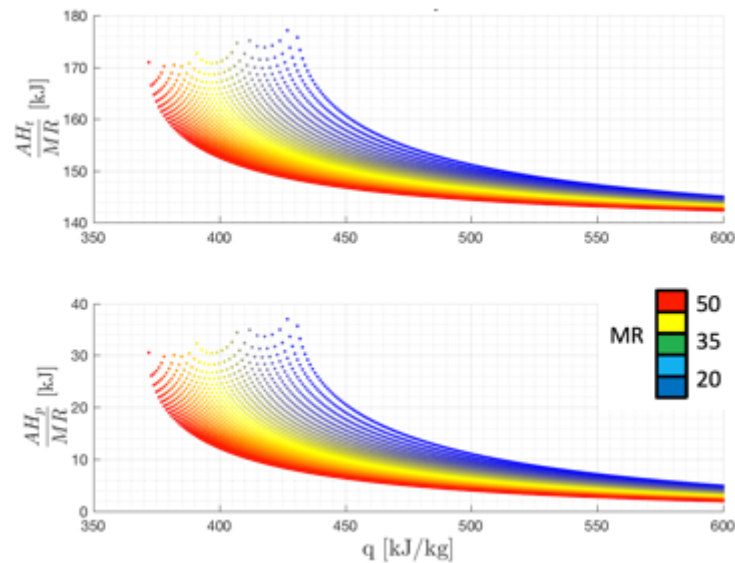

Figure 5.11: Turbine and pump specific work vs heat addition to the working fluid, at $M_0 = 2.1$ and $\pi_f = 2.5$
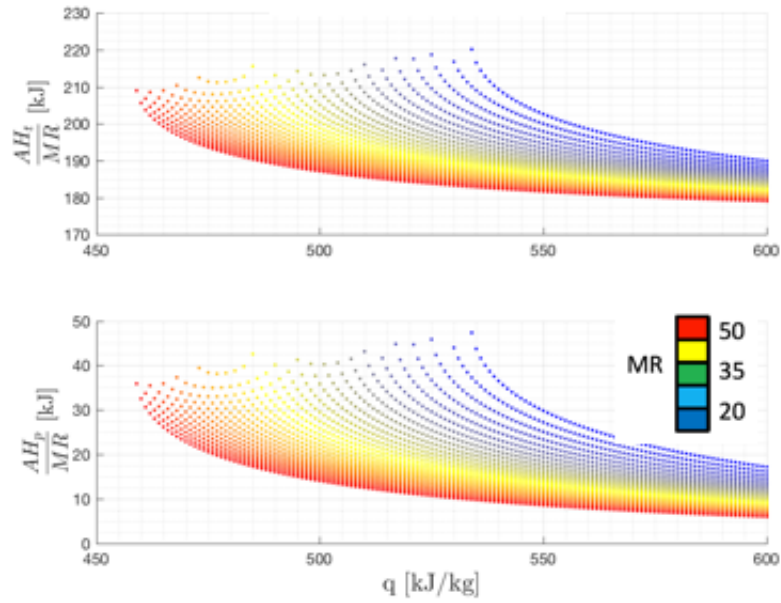
Figure 5.12: Turbine and pump specific work vs heat addition to the working fluid, at $M_0 = 2.1$ and $\pi_f = 3$

Thereupon, results of point 4, $M_0 = 3.2$ and h = 22 km will be exposed.
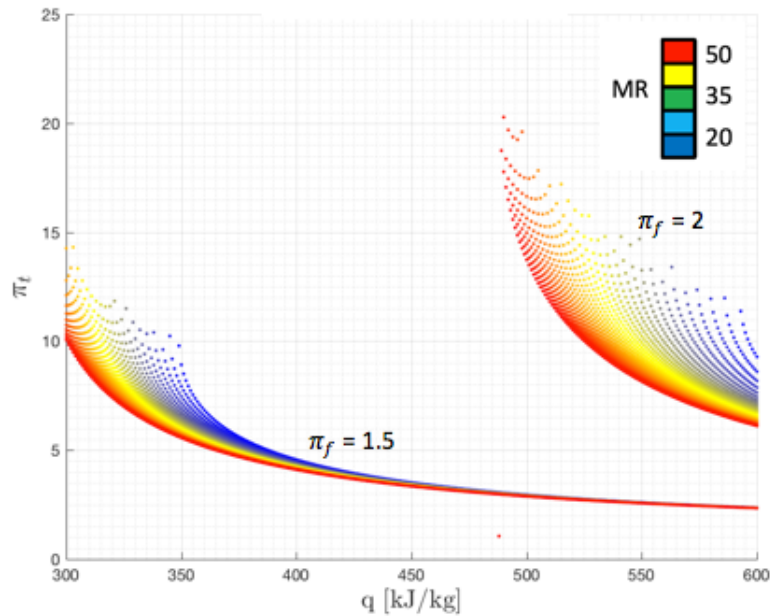

Figure 5.13: Turbine expansion ratio vs heat addition to the working fluid, at $M_0 = 3.2$

Figure 5.13 show clearly what it is already commented above. When the Mach number is increasing, the curves representing different fan compression ratios are further between them, establishing a clear range of fan operation in the cycle, reducing it to values close

to the unit. It has to be taken into account that the ATR cycle is designed to operate up to Mach 4.5, where the DMR is ready to be used. At Mach $= 3.2$, the DMR is starting to work, but with α_c^{HSI} very lows. Progressively, this value will be increasing, and consequently α_c^{LSI} will be decreasing, so this transition will be complete at Mach 4.5, when the π_f is equal to 1.
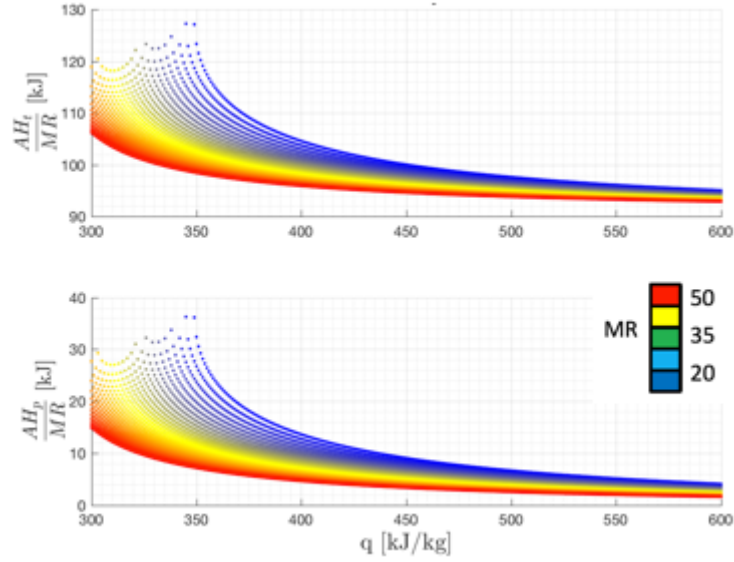

Figure 5.14: Turbine and pump specific work vs heat addition to the working fluid, at $M_0 = 3.2$ and $\pi_f = 1.5$
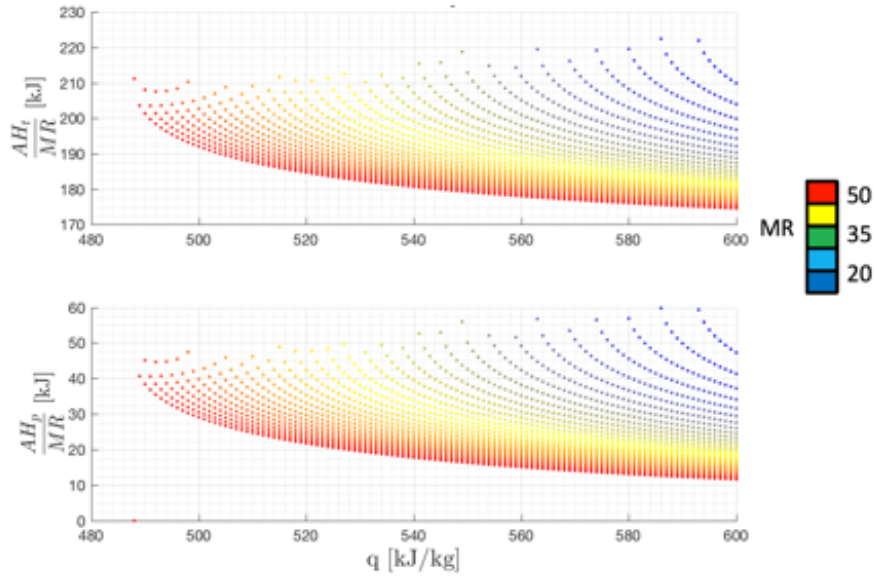

Figure 5.15: Turbine and pump specific work vs heat addition to the working fluid, at $M_0 = 3.2$ and $\pi_f = 2$

Figures 5.14 and 5.15 show the specific works for this flight regime. As stated before, the fan pressure ratio is governing these regimes, in which the stable behavior is near to the unity. The tendencies that have been constant along all the study can be observed in Figure 5.14. Nevertheless, these tendencies are similar to the previous ones when decreasing the π_f. If it is not reduced and maintained constant, as shows Figure 5.15, a huge mixture ratio is needed to satisfy a reasonable turbine specific work, while decreasing this parameter conducts the cycle to provide a big amount of heat to the fuel flow. So, it is more interesting to continue decreasing the π_f until the ATR engine is not working anymore ($\pi_f = 1$).

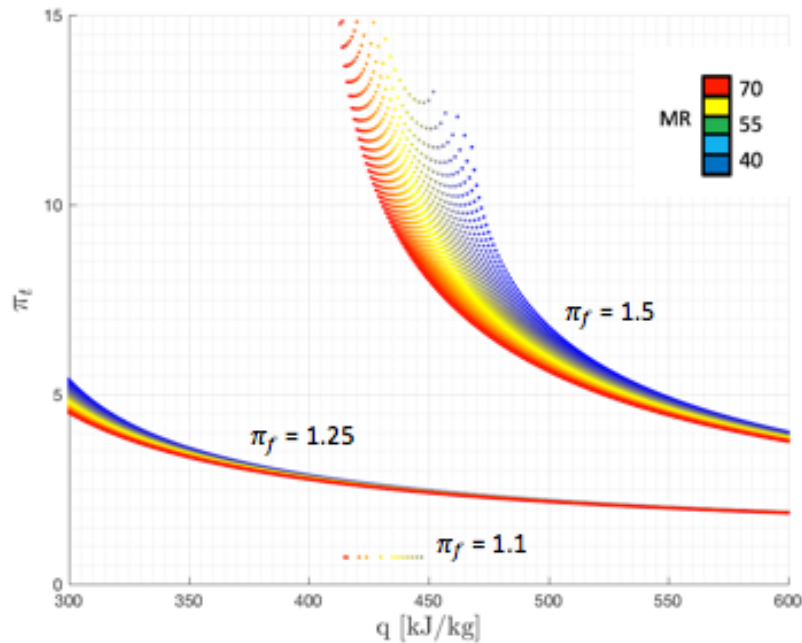Results from point 5, $M_0 = 4$ and h = 24 km, are exposed below.

Figure 5.16: Turbine expansion ratio vs heat addition to the working fluid, at $M_0 = 4$

Following the tendency of reducing the π_f, it is clear that the lower value this parameter has, the lower turbine expansion ratio. It can be observed in Figure 5.16 that the π_t are very low compared with the previous ones, logically. Moreover, if the fan pressure ratio would be 1.1, the π_t would be very close to the unity, as well. Take into account that the only purpose of the turbine is driving both the pump and the fan, and the pump does not consume much work, so it is clear that the turbine will be stopping its task very soon (when reaching the point $M_0 = 4.5$). Then, the operational point for this condition will be around $\pi_f = 1.25$, because the curve representing this point is able to operate in the whole range of heat addition, so there is no great dependency of the heat exchangers, case that is actually happening in the point $\pi_f = 1.5$.

Figures 5.17 and 5.18 show the influence of the heat addition on the turbine and pump specific works, varying the mixture ratio. As commented before, the curve that
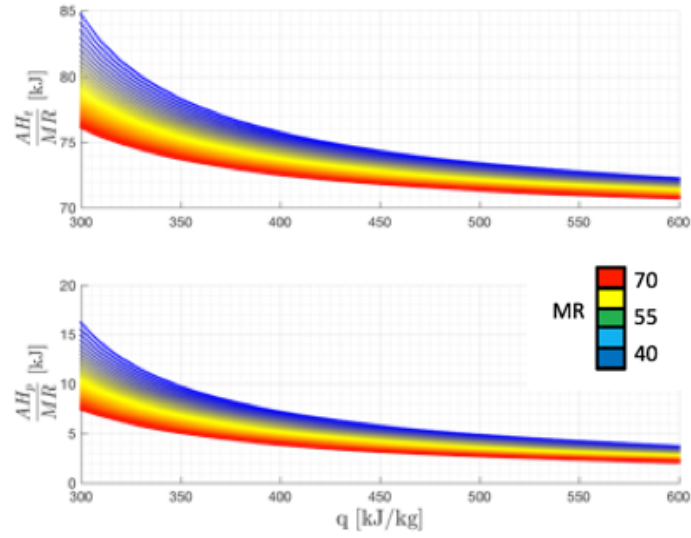
Figure 5.17: Turbine and pump specific work vs heat addition to the working fluid, at $M_0 = 4$ and $\pi_f = 1.25$

corresponds to $\pi_f = 1.25$ is similar to the previous regimes, and allows more freedom when designing the ATR cycle. Nevertheless, increasing the fan pressure ratio would lead to need more turbine expansion ratio and heat addition, so the tendency of decreasing the π_f when the flight velocity increases is perfectly justified. Moreover, this is the desirable condition; the transition between the ATR and the DMR is being carried out progressively, with no discontinuities, and end up switching off the ATR engine softly, with no abrupt changes.
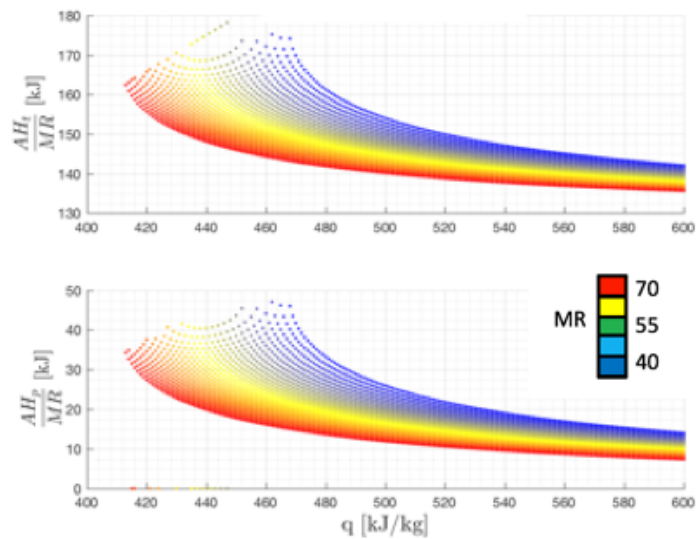

Figure 5.18: Turbine and pump specific work vs heat addition to the working fluid, at $M_0 = 4$ and $\pi_f = 1.5$

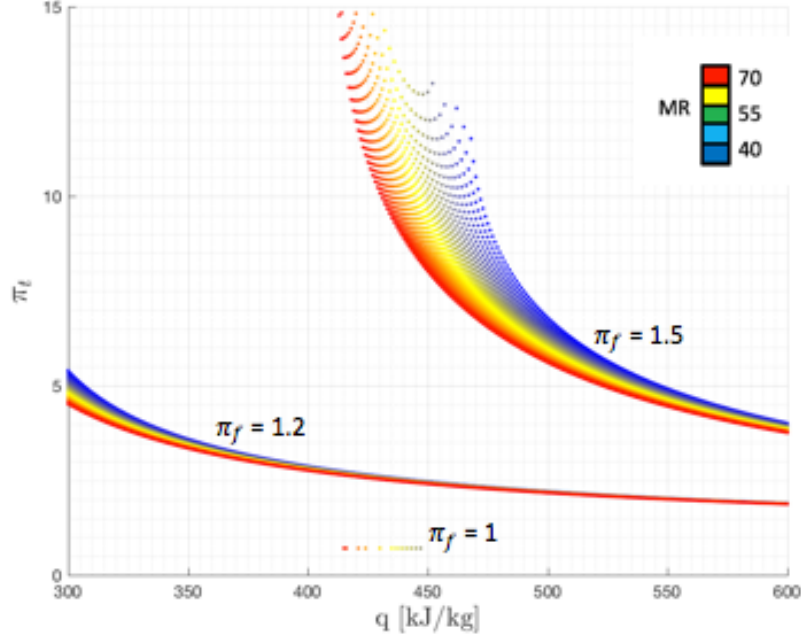Finally, results from point 6, $M_0 = 4.5$ and h = 25.6 km, are exposed below.

Figure 5.19: Turbine expansion ratio vs heat addition to the working fluid, at $M_0 = 4.5$

Figure 5.19 shows the π_t needed at $M_0 = 4.5$ with a certain amount of heat extracted by the heat exchangers and added to the flow. Following the tendency of the previous cases, it can be observed that the fan pressure ratio that is admited in this part of the trajectory is very low. In fact, this point corresponds to $\pi_f = 1$, but some more cases are modeled in case of need of certain compression to the air. As the figure show, the correct value of fan compression ratio for this point would go from 1 to 1.2, in which the heat addition is not very big, and the π_t has a very low value. Nevertheless, it is important to remark that the engine is thought to establish a $\pi_f = 1$ at this point, so this is the final working point of the ATR engine.

Figures 5.20 and 5.21 show the specific works versus the heat addition and the mixture ratio. It is clear that the curves corresponding to $\pi_f = 1.4$ are not a good working point, due to the large disparity of results when modifying the mixture ratio. Nevertheless, if the fan pressure ratio were not equal to the unity, the point of $\pi_f = 1.2$ is a stable point to work with. Tendecies are similar than in previous cases, but with a considerable reduction of turbine specific work.

As a conclusion for this section, it can be stated that the turbine specific work is maximum within values from $M_0 = 1.7$ to $M_0 = 2.1$, and then it starts to decrease, along with the fan pressure ratio, which will be decreasing little by little until it becomes the unity, in the point $M_0 = 4.5$. The heat addition is interesting because this allows the engine reduce its size and weight, due to the less turbine expansion ratio that is needed to satisfy the cycle demand. As well, increasing the mixture ratio leads to need less π_t, due to the reduce of fuel massflow increases the turbine inlet temperature and leads to a
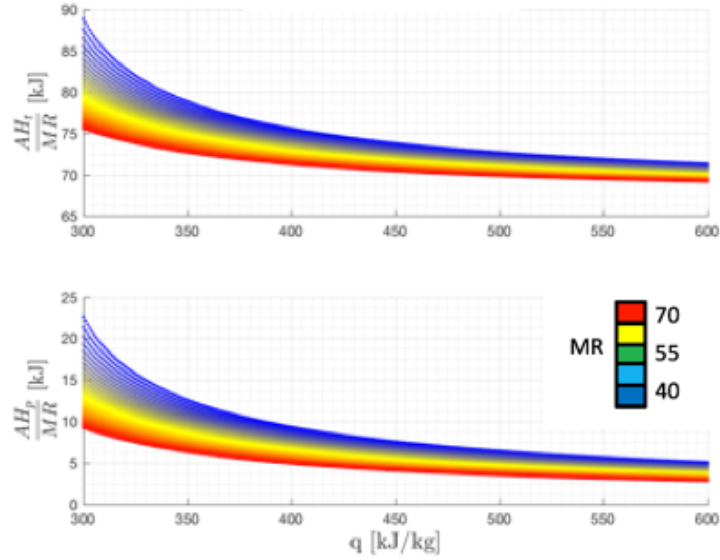
better expansion.

Figure 5.20: Turbine and pump specific work vs heat addition to the working fluid, at $M_0 = 4.5$ and $\pi_f = 1.2$
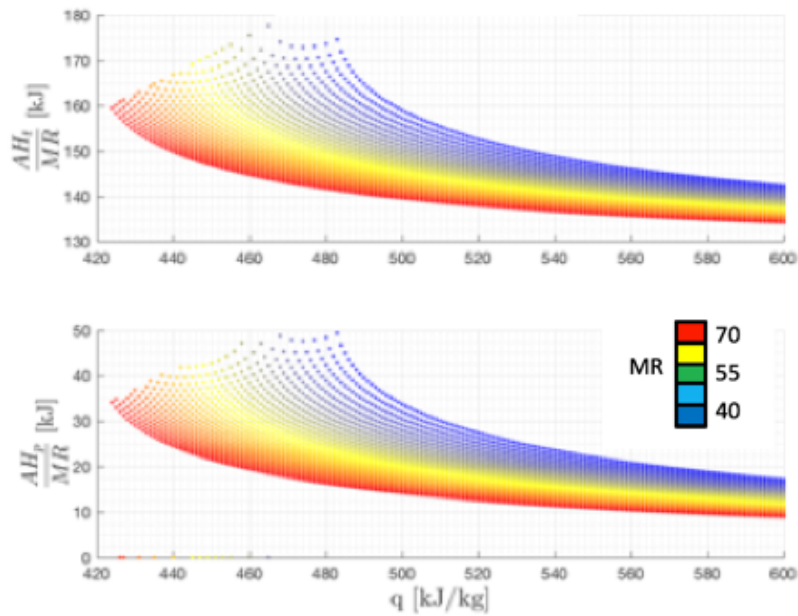

Figure 5.21: Turbine and pump specific work vs heat addition to the working fluid, at $M_0 = 4.5$ and $\pi_f = 1.4$

The operational range study has come to the end, and now it is time to comment the engine performance along the trajectory computed in this last study (Table 5.3).

5.3 Engine performance

This section is focused on the study of the specific impulse and specific thrust, depending on the mixture ratio and the fan pressure ratio. Maximizing these two performance parameters is what it is intended when designing the ATR engine. That is why its study is very important for the developing of this engine, so a study along the trajectory of the MR2 will be exposed, following the same points the Table 5.3 showed.

To start with, the influence of each parameter will be analyzed using the Figure 5.22.
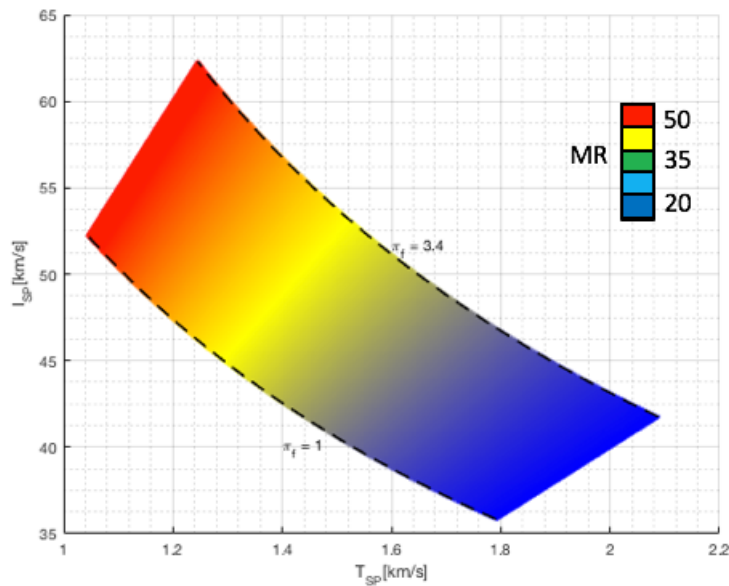

Figure 5.22: Engine performance at $M_0 = 1.1$

Figure 5.22 shows the performance parameters specific thrust versus specific impulse with different mixture ratios and fan compression ratios. As it is shown in the image, both performance parameters show a trade-off between maximizing either the specific thrust or the specific impulse. The curve, at a constant π_f, is decreasing the specific impulse when increasing the specific thrust. As well, at low mixture ratios the specific thrust is maximum, due to the fact that the less air massflow there is in the engine (less MR), with constant thrust, the higher value for the specific thrust. At the same time, if the MR is high, it means that the fuel massflow is low, so it provokes that, at constant thrust, the specific impulse increases its value. The only way to make both parameters higher at the same time is increasing the fan pressure ratio. The Figure 5.22 shows an increase in both variables when passing from $\pi_f = 1$ to $\pi_f = 3$. Nevertheless, it is proven in the previous chapter that the increase in the fan pressure ratio could lead to a very high heat addition need, maybe impossible to satisfy by the heat exchangers. Then, as stated before, a trade-off between these two parameters and with the turbomachinery variables is needed when designing the operational points of the engine.

Next, the same results but for the rest of the points of Table 5.3 are going to be shown.
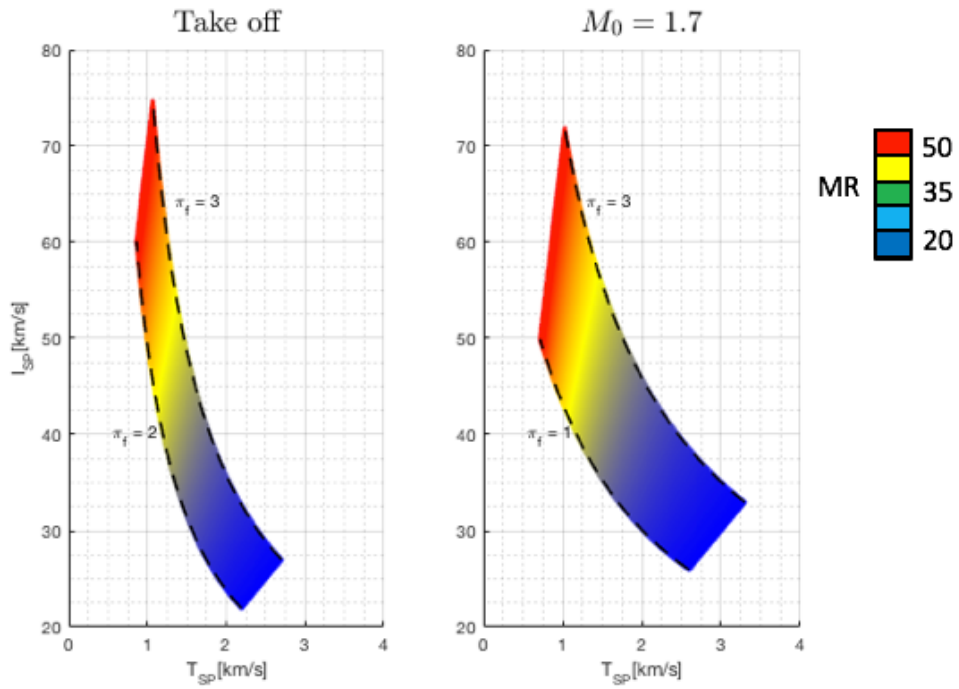
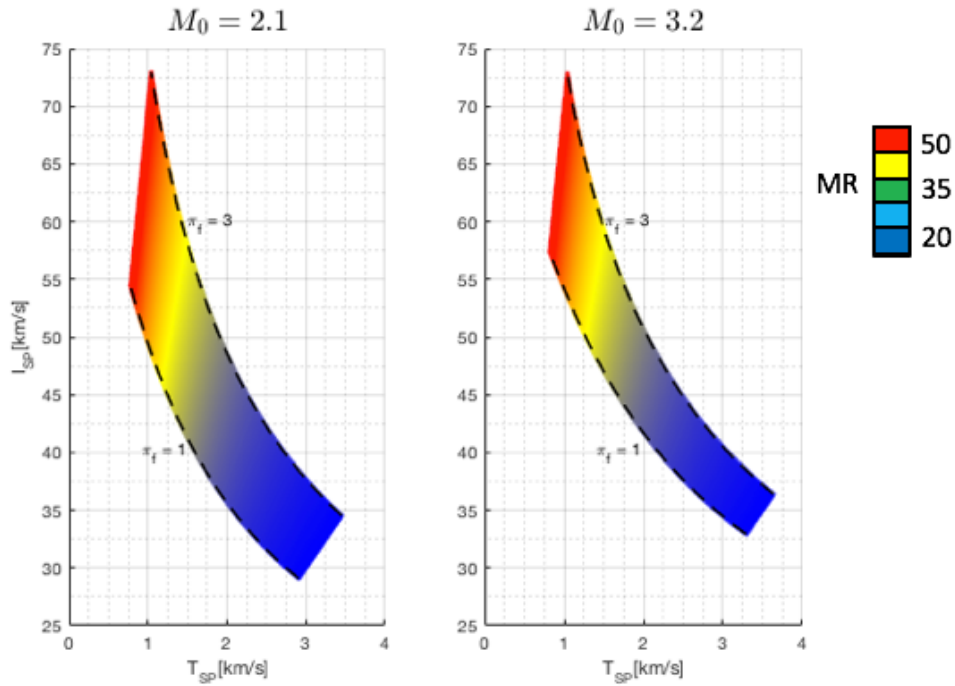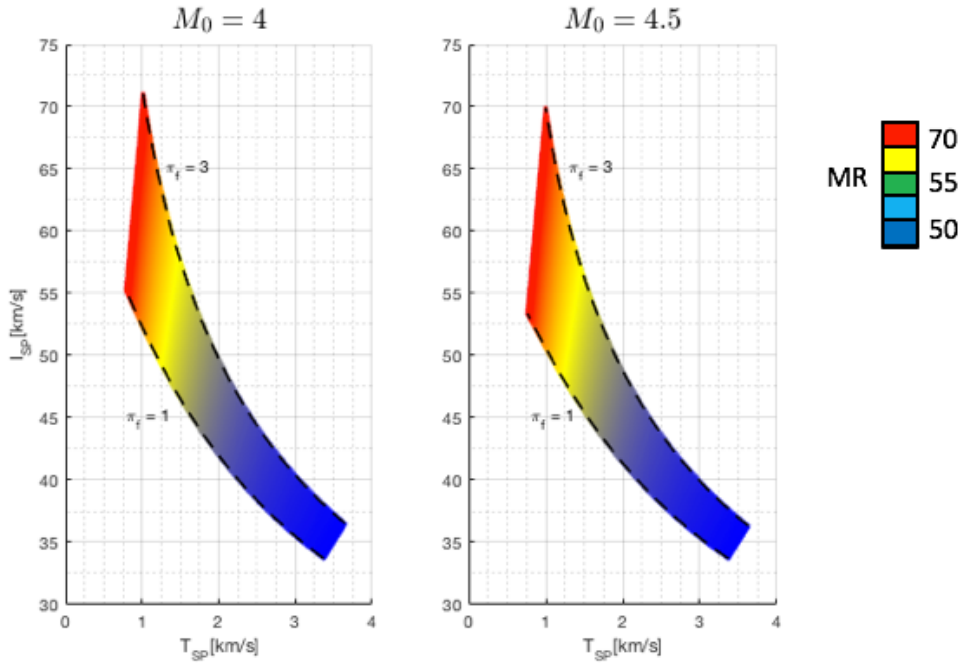Figure 5.23: Engine performance at take off and $M_0 = 1.7$

Figure 5.24: Engine performance at $M_0 = 2.1$ and $M_0 = 3.2$

Figure 5.25: Engine performance at $M_0 = 4$ and $M_0 = 4.5$

Figures 5.23, 5.24 and 5.25 show, along with the Figure 5.22, that both specific thrust and specific impulse present the same order of magnitude, even quite similar values, when changing the flight condition. Although there is a minimum variation, every operational point shows the same tendency and similar values. This is a very important characteristic of the ATR engine; it is able to present more or less the same behavior over the whole trajectory, maintaining the performance parameters almost constant, if the mixture ratio and the fan pressure ratio are chosen correctly. It is necessary to remind that the performance parameters are independent from the pressure drop and the heat addition by the heat exchangers, but dependent just of mixture ratio and π_f (translated to the chamber total pressure). As a result, if these two parameters are maintained more or less constant, depending of the flight regime, the performance will be quite constant.

5.4   Nozzle throat area

This study is focused on the determination of the minimum nozzle area the engine needs to have, in order to satisfy the mission specifications. Until this moment, the cycle has been established without taking into account the amount of massflow that is going to circulate throughout the engine. By calculating the performance parameters, the engineer can have a general idea of the needs of the engine, but then, sizing the engine and calculating the net thrust, the air and fuel massflows and the nozzle area are the next step, taking into account the mission requirements.

This section will be focused on the nozzle area in subsonic and supersonic regime as a function of the mixture ratio and fan pressure ratio, and then it will be shown the bleeding

influence on the area selection. Finally, another graph will be shown as a function of the turbine work.

First, the nozzle area as a function of fan pressure ratio and mixture ratio, for both subsonic and supersonic regimes are shown in Figures 5.26 and 5.27.
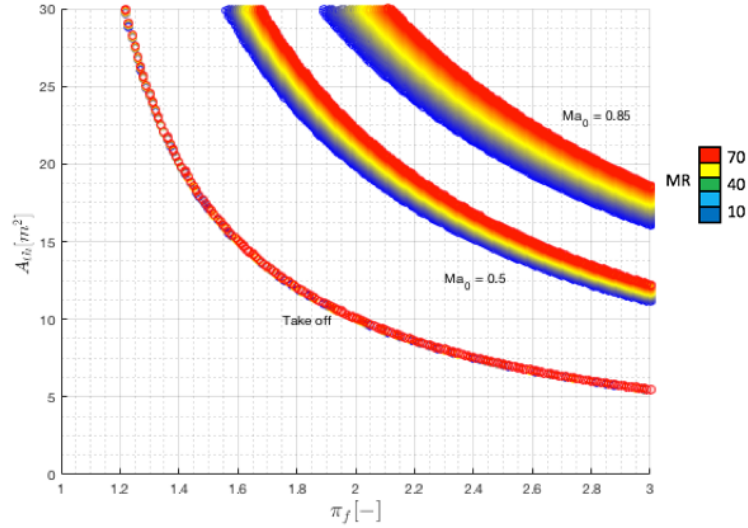
Figure 5.26: Nozzle throat area vs π_f and MR in subsonic regime
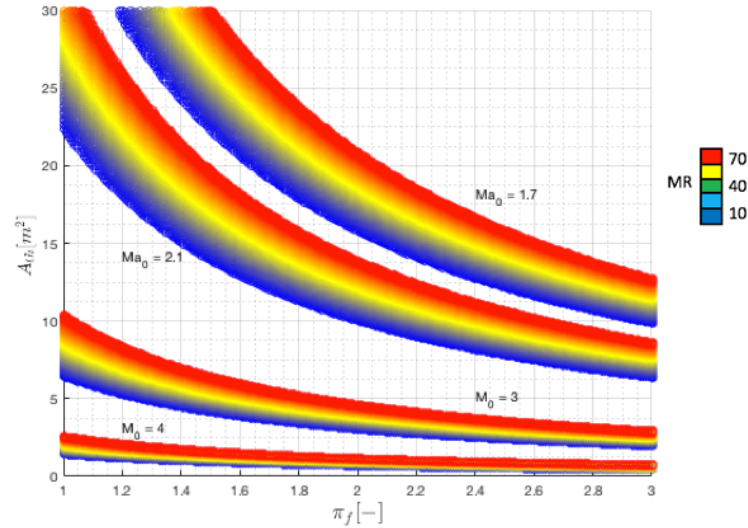
Figure 5.27: Nozzle throat area vs π_f and MR in supersonic regime

As shown in Figures 5.26 and 5.27, the nozzle area increase its value along the trajectory (higher flight Mach, higher altitude) because the ambient static pressure decreases. As well, it is clear that the mixture ratio has an important role when the flight velocity increases, being independent from the nozzle area at low velocities, such as take off. That

is because the nozzle exhaust velocity increases with the mixture ratio, so the area needed for that massflow is higher than at lower velocities. On its behalf, the fan pressure ratio provokes the area to reduce its value because the higher pressure there is in the combustion chamber, the higher the density is; for a constant massflow, the area has to be reduced to make the process stationary.

As proven in Chapter 3.3, some bleeding is needed for the correct functioning of the engine, due to the fact that the ATR produces more thrust than the required in the MR2 mission. As a result, a study has been performed to investigate how much bleeding is necessary as a function of the fan pressure ratio, and the area needed for that mission.
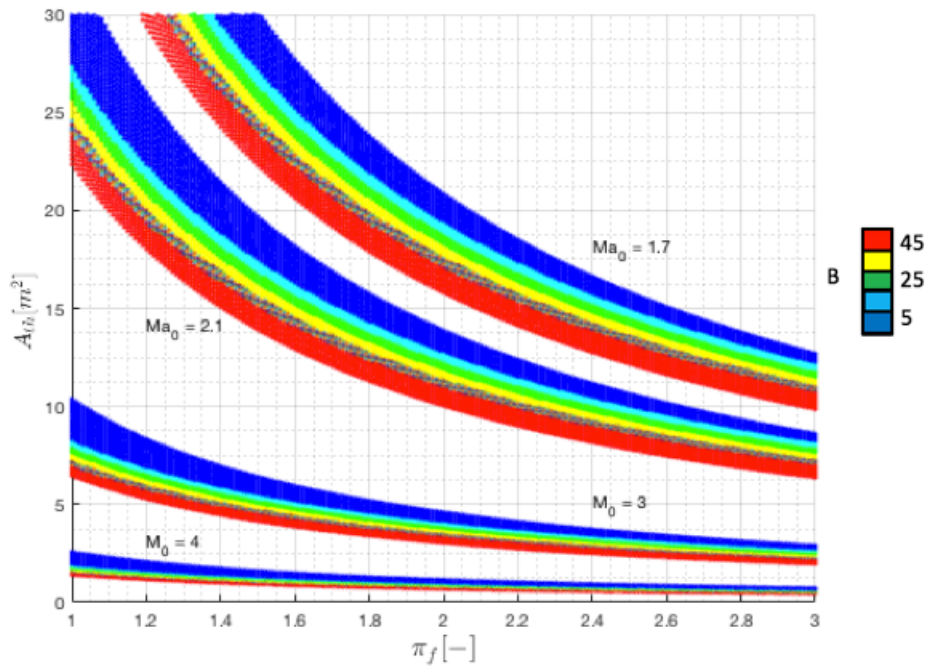
Figure 5.28: Nozzle throat area vs π_f and bleeding ratio

As Figure 5.28 shows, the bleeding is taking place in points where the mixture ratio is low, as Figure 5.27 showed. This is because the specific thrust is maximum when the mixture ratio is low, as it was exposed in Section 5.3. The amount of bleeding is a measure of excess of thrust, and it can be written as

$$B = 1 - \frac{T_{sp}^{min}}{T_{sp}} \tag{5.1}$$

Then, when the specific thrust is adopting high values, more bleeding is necessary to obtain the desired thrust for the mission.

Finally, the last study of this section is dedicated to study the turbine work that is necessary to drive the turbomachinery, as a function of the fan compression ratio and the nozzle area, both in regime subsonic and supersonic.

Figure 5.29: Nozzle throat area vs π_f and turbine work in subsonic regime
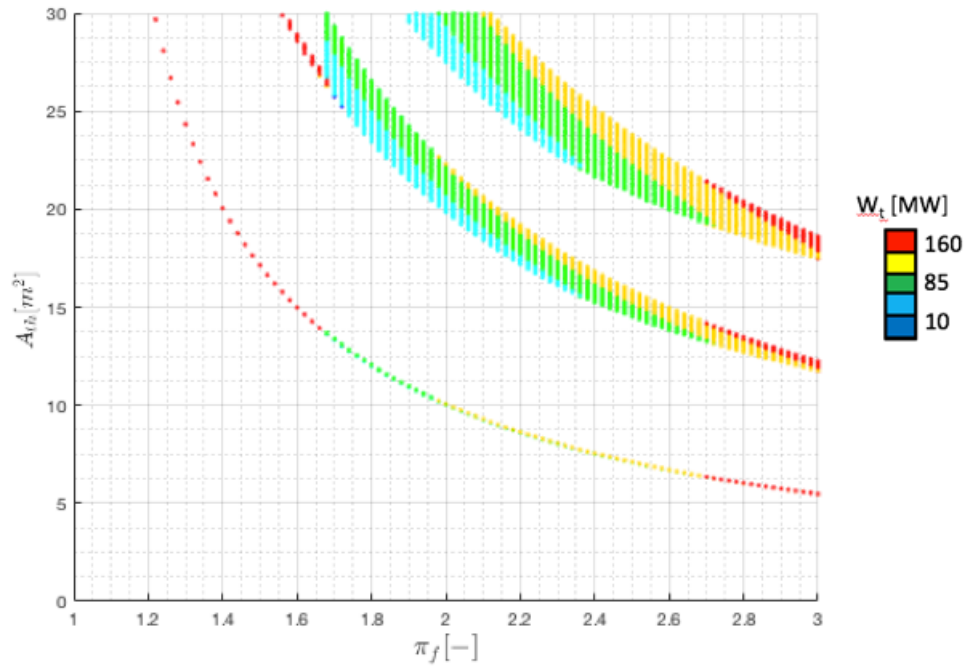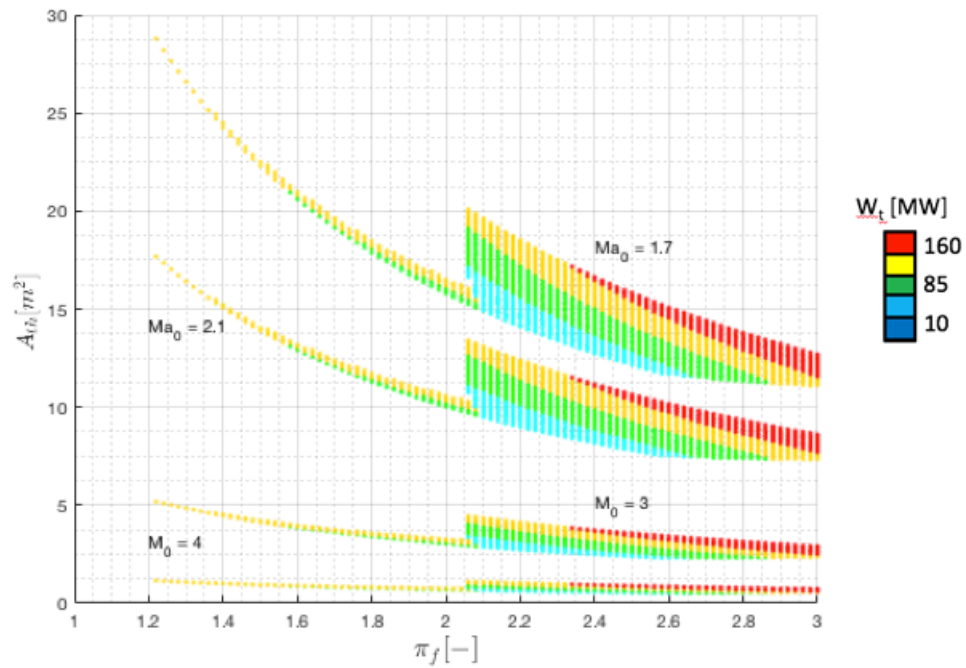

Figure 5.30: Nozzle throat area vs π_f and turbine work in supersonic regime

Figures 5.29 and 5.30 show the nozzle throat area versus the π_f, as a function of the turbine work, for the subsonic and supersonic regime, respectively.

When the throat area and the compression ratio are increasing, the turbine load is increasing as well. The power required by the turbomachinery is quite sensitive to the throat area when the engine is flying at low Mach numbers. Then, when the $M_0 = 3$ point is reached, the load is almost independent of the throat area, and the fan pressure ratio is the dominant parameter, talking about the supersonic regime. Consequently, the optimum configuration leads to the minimum turbine work, so these points will be the ones chosen for the operational line, taking into account the heat addition that would be possible to achieve by the heat exchangers.

5.5 Turbine work vs π_f

Finally, the last study of this document focuses its interest in the turbine load, as a function of fan pressure ratio and mixture ratio, both in subsonic and supersonic regimes.
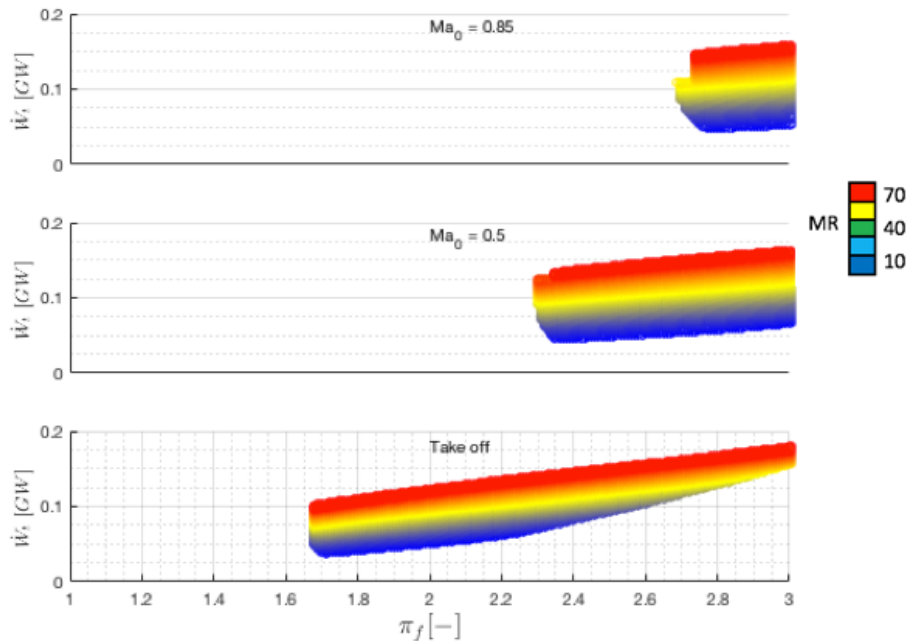
Figure 5.31: Turbine power vs. fan pressure ratio and mixture ratio, at subsonic regime

Figures 5.31 and 5.32 show the turbine work vs. fan pressure ratio and mixture ratio. As it is exposed in the images, the turbine load increases with the mixture ratio, due to the fact that the air massflow through the fan is increasing, so this component needs more work to drive all that flow. On its behalf, increasing the fan pressure ratio leads to an augment of the power provided by the turbine. This is something logical, if the reader takes into account that the more compression power the fan requires, the more power the turbine has to produce to satisfy that power balance. Finally, it can be observed that the maximum power demand corresponds to the areas close to $M_0 = 2$, as it was predicted in the last studies. When the velocity keeps increasing, the power demand is lower due to the fan pressure ratio is lower as well.
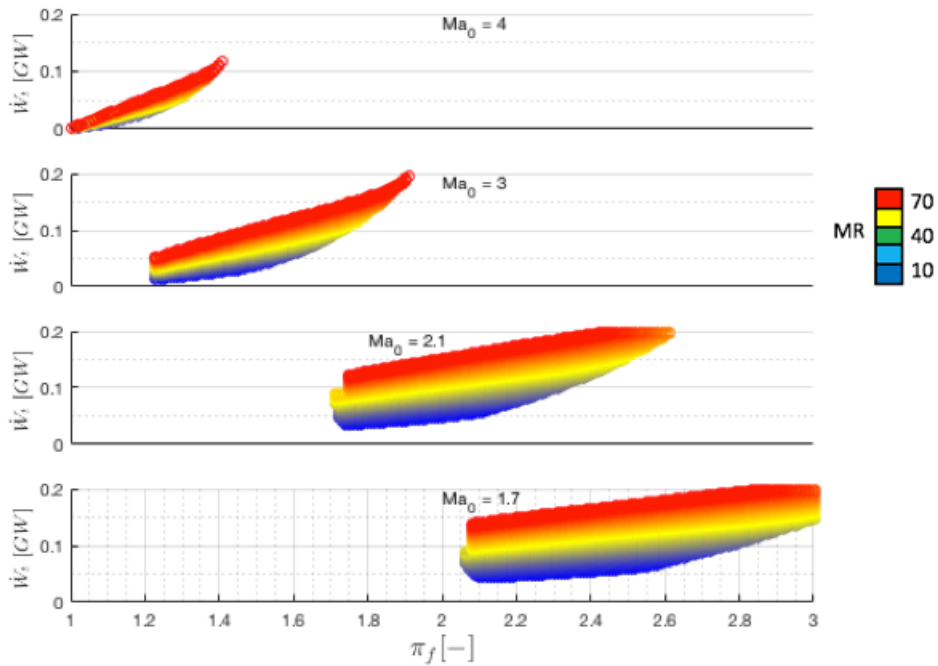
Figure 5.32: Turbine power vs. fan pressure ratio and mixture ratio, at supersonic regime

Five studies have been exposed in this document, and now, being conscious of the behavior of the engine, the next step is to choose the operational points of the engine along the whole trajectory. These operational points are chosen by a numerical algorithm of optimization, made by a computer, but here it can be predicted which points they will be. To start with, the maximum turbine power and the maximum nozzle area have to be chosen. Then, it will impose a restriction in which many points that are exposed in these figures will be out-of-range. Then, it has to be taken into account that it is preferable to choose a mixture ratio close to the stoichiometric ($MR = 34.33$), in order to maximize the heat transfer made to the walls and then to the heat exchangers. This is an important restriction too: it has to be specified how much heat the heat exchangers can extract and add to the fuel, due to this is a very important condition to minimize the turbine power. Considering all these restrictions, the operational line of the engine has to be established, but this is proposed for future works.

6
Financial estimation

This chapter is dedicated to detail the economic estimation about the total budget of the project. There are several fields that contribute to the final amount that have made possible the realization of this work:

- The equipment used consists on the user computer, valuated in 2.000 €, and the supercomputers that are present in the Von Karman Institute, which have a cost of 10.000 €.

- This project has been developed in the context of an internship, whose fellowship has consisted on 350 € per 5 months, so the total sum rose to 1.750 €.

- The programs used for this project have been Matlab and EcosimPro. These are not open software, they require a license for being able to work with them, so these are also included in the budget. The license for EcosimPro is 10.000 €, and the Matlab one, 800 €, according to their official webpage.

- Finally, the project has been supervised by a research engineer. The project has taken 5 months, and the supervisor has dedicated 2 hours per week to the study, so he has employed 40 hours in it. If the engineer is paid 80 € per hour, it can be estimated that the derived cost of receiving help of such a qualified person is 3.200 €.

Table 6.1 sums up all the costs that contribute to the final sum.

Concept	Quantity
Equipment	12.000 €
Fellowship	1.750 €
Licenses	10.800 €
Supervisor	3.200 €
Total	**27.750 €**

Table 6.1: Project's financial estimation

7
Conclusions and future work

7.1 Conclusions

The Air Turbo-Rocket Expander engine has been introduced in this document as a combined cycle for high-speed propulsion, destined to commercial flights up to Mach 8 in the aircraft designed by LAPCAT, MR2. This combined cycle is characterized by four meaningful parameters: fan pressure ratio, mixture ratio, heat extracted and pressure loss in the heat exchangers, while the turbomachinery efficiencies and the flight condition remain constant. In addition, it has been proven that the performance parameters are only determined by two variables: fan pressure ratio and mixture ratio.

Some studies related with supersonic engines such as turbojet and ramjet have been exposed. These studies have been made in the numerical software EcosimPro, which is a powerful tool to develop engine models by an object-orientated language, in which every component has its own code and functions, and interact with other components by the ports connection. In addition, this software is valid for steady, transient and optimization calculations.

The Air Turbo-Rocket Expander engine has been modeled analytically and several studies have been proposed in this document along the whole trajectory this engine has, until it is switched off and the DMR operates at 100%. This trajectory goes from take off to Mach 4.5, and there are several changes along this trajectory. First, the fan compression ratio increases up to 3, at $M_0 = 2$, approximately, and then starts to lower its value until it reaches the unity. As it is proportional to the turbine power, this component has the same behavior. On another note, the supersonic regime needs a bypass duct not to overcome the specific thrust the engine needs. There is a balance between the bleeding and other meaningful parameters, such as mixture ratio or fan pressure ratio, in order to choose the correct value in each point of the trajectory.

The ATR engine is designed within two main characteristics: maximize both specific thrust and specific impulse. This goal represents a trade-off between both of the two parameters, and they depend solely on the fan pressure ratio and the mixture ratio. It has been proven that increasing the π_f both of them increase. However, increasing the fan compression ratio would cause other problems, such as lack of turbine power to supply to the fan or lack of heat addition to the fuel flow.

The operational points that will be set for the trajectory of the MR2 have to be chosen taking into account the restrictions the engine presents. First of all, the mixture ratio should be good enough to guarantee an efficient combustion in which a considerably amount of heat is liberated, in order the heat exchangers to extract it and transfer it to the fuel flow. According to this, the heat addition will determine the maximum turbine power the cycle needs. One of the challenges of the ATR is to develop some good heat exchangers to reduce the turbine size and weight and make the engine lighter, more compact, and more efficient. In addition, two more restrictions are the maximum area nozzle and the maximum turbine work possible for the engine, so these will determine the frontier between

real possible operational working points and just mathematical solutions that are not able to be implemented in real engines.

7.2   Future work

This proyect is so huge that many organizations are working in make the combined cycles for high speed propulsion a realty. As a conclusion, there is so much work to do for the future 20-30 years until this kind of engine becomes a reality. Nevertheless, it can be established as future work:

- The selection of the operational line of the engine along the whole trajectory, and its optimization.

- The developing of reliable models for the fan, the turbine, the pump, the heat exchangers and the nozzle.

- The developing of the complete model in EcosimPro and its simulation.

- The specification of how the transition between the ATR engine and the DMR engine is going to be performed.

Bibliography

[1] Empresarios Agrupados, Astrium, Cenaero, Kopoos, and VKI. *ESPSS - European Space Propulsion System Simulation - EcosimPro Libraries User Manual*. September 2012.

[2] Victor Fernandez Villace. Simulation, Design and Analysis of Air–Breathing Combined–Cycle Engines for High Speed Propulsion.

[3] Timothy Barber, Brian Maicke, and Joseph Majdalani. Current State of High Speed Propulsion: Gaps, Obstacles and Technological Challenges in Hypersonic Applications. American Institute of Aeronautics and Astronautics, August 2009.

[4] H. Sänger Kuczera Koelle, J. E. Space Transportation System Status, 1998.

[5] D. T Pratt Heiser, W. H. *Hypersonic airbreathing propulsion*. AIAA Education Series. 1994.

[6] J Steelant. LAPCAT: High-Speed Propulsion Technology.

[7] John Beyer, Julian Cooper, Gerald Holden, François Nectoux, Nancy Ramsey, David Schorr, Tony Thompson, Andrew White, and Scilla McLean. North Atlantic Treaty Organisation. In Scilla McLean, editor, *High Speed Propulsion: Engine Design - Integration and Thermal Management*, pages 204–233. Palgrave Macmillan UK, London, 1986.

[8] Victor Fernandez-Villace and Guillermo Paniagua. Numerical Model of a Variable-Combined-Cycle Engine for Dual Subsonic and Supersonic Cruise. *Energies*, 6(2):839–870, February 2013.

[9] F Jivraj, R Varvill, A Bond, and G Paniagua. The Scimitar Precooled Mach 5 Engine.

[10] History of Aviation, 2010.

[11] Nancy McNelis and Paul Bartolotta. Revolutionary Turbine Accelerator (RTA) Demonstrator. In *AIAA/CIRA 13th International Space Planes and Hypersonics Systems and Technologies Conference*. American Institute of Aeronautics and Astronautics.

[12] Jinho Lee, Ralph Winslow, and Robert J Buehrle. The GE-NASA RTA Hyperburner Design and Development. page 22, 2005.

[13] Roger W Luidens. An Analysis of Air-Turbo Rocket Engine Performance including effects of component changes. Technical Report RM E55H04a, Lewis Flight Propulsion Laboratory, NACA, Cleveland, April 1956.

[14] Giuseppe Bussi, Guido Colasurdo, and Dario Pastrone. Analysis of air-turborocket performance. *Journal of Propulsion and Power*, 11(5):950–954, September 1995.

[15] Nobuhiro Tanatusgu, Tetsuya Sato, Yoshihiro Naruo, Takeshi Kashiwagi, Tomoaki Mizutani, Toshiyuki Monji, and Kenji Hamabe. Development study on ATREX engine. *Acta Astronautica*, 40(2-8):165–170, January 1997.

[16] Preston Carter, Vladimir Balepin, Terry Spath, and Christopher Ossello. MIPCC Technology Development. In *12th AIAA International Space Planes and Hypersonic Systems and Technologies*, International Space Planes and Hypersonic Systems and Technologies Conferences. American Institute of Aeronautics and Astronautics, December 2003.

[17] R Freese Balepin et al, V. Rocket Augmentation for Combined Cycle Turboaccelerator Jet Engine. December 2007.

[18] Dr Vladimir Balepin. High Speed Propulsion Cycles.

[19] Ed Envia. Engine Intake Aerothermal Design: Subsonic to High Speed Applications. Lectures Series - Von Karman Institute, National Aeronautics and Space Administration, 2011.

[20] W. A. Kuhrt. Turborocket Engine.

[21] G. T. Peters N. C. Newington and N. C. Rice. Regenerative Expander Engine, March 1966.

[22] N. Rackemann T. Fuhrmann and S. Krügen. EcosimPro ATR-EXP and ATR-GG modeling and feasibility study for the ESTEC Mach 8 concept. Cologne - Germany, 2011.

[23] COSAP Sizing Tool Application for ATR Cycle. LAPCAT II Derivable D3.3.3, 2009.

[24] Preliminary Mach 8 Turbo-Based /DMR Vehicle Analysis: Conceptual Design of a Dorsal-Type Vehicle: LAPCAT-MR2. LAPCAT II Derivable D3.1.4, 2009.

[25] Modelling Language.

[26] L. R. Petzold. DASSL: Differential Algebraic System Solver. Technical Report, Sandia National Laboratories, Livermore, CA, 1983.

[27] Math. Algorithms & Simulation Guide.

[28] Alberto Jorrín. EcosimPro and its EL Object-Oriented Modeling Language. page 10.

[29] Romain Gérard. *Waterhammer simulations in an EcosimPro/ESPSS environment.* PhD thesis, von Karman Institute for Fluid Dynamics, Brussels, Belgium, June 2013.

[30] M. E Thomas and J. A. Bossard. The influence of turbomachinery characteristics on Air Turbo Rocket engine operation. Huntsville, ALA, 2000.

[31] Kirk Christensen. Air Turborocket/Vehicle Performance Comparison. *Journal of Propulsion and Power*, 15(5):706–712, September 1999.

[32] A. M. J Lardellier and R. P. M. Thetiot. Combined Turborocket and Ramjet Propulsion Unit.

[33] M. Albers, D. Eckardt, P. A. Kramer, and N. H. Voss. Technology preparation for hypersonic air–breathing combined cycle engines. American Institute of Aeronautics and Astronautics, 1989.

[34] Kousuke Isomura, Junsuke Omi, Nobuhiro Tanatsugu, Tetsuya Sato, and Hiroaki Kobayashi. A feasibility study of a new ATREX engine system of aft-turbine configuration. *Acta Astronautica*, 51(1):153 – 160, 2002.

[35] Tetsuya Sato, Hideyuki Taguchi, Hiroaki Kobayashi, Takayuki Kojima, Katsuyoshi Fukiba, Daisaku Masaki Okai, Keiichi, Kazuhisa Fujita, Motoyuki Hongo, and Shujiro Sawai. Development study of a precooled turbojet engine. *Acta Astronautica*, 66(7):1169–1176, April 2010.

[36] C Meerts and J Steelant. Air Intake Design for the Acceleration Propulsion Unit of the LAPCAT-MR2 Hypersonic Aircraft. page 18, 2013.

[37] I Rodríguez Miranda. Modeling, Analysis and Optimization of the Air Turbo Rocket Expander Engine.

[38] Johan Steelant. Sustained Hypersonic Flight in Europe: First Technology Achievements within LAPCAT II. In *17th AIAA International Space Planes and Hypersonic Systems and Technologies Conference*. American Institute of Aeronautics and Astronautics.

[39] Empresarios Agrupados, Cenaero, Kopoos, Astrium, and VKI. *ESPSS - European Space Propulsion System Simulation - Software Verification and Validation Plan*. 2013.

[40] GasTurb GmbH . *GasTurb 12*. 2015.

[41] Victor Fernandez Villace, G Paniagua, and I. Rodriguez Miranda. Thermal evaluation and cooling channels design - ATR cycle design. Theme 7: Transport. VKI, August 2013.

[42] Victor Fernandez Villace. Refined engine cycle analysis, results and preliminary dimensions - Integral performance of the MR2 propulsive plant in the Mach range from 1.5 to 4.5. Theme 7: Transport. VKI, August 2013.